

The Role of Elevated Ducting for Radio Service and Interference Fields

H.T. Dougherty

E.J. Dutton



U.S. DEPARTMENT OF COMMERCE
Malcolm Baldrige, Secretary

Dale N. Hatfield, Acting Assistant Secretary
for Communications and Information

March 1981

TABLE OF CONTENTS

	Page
ABSTRACT	
1. INTRODUCTION	1
1.1 Degradation of Service Fields	2
1.2 Enhancement of Interference Fields	2
2. DUCTING STRUCTURES	8
2.1 Ducting	9
2.2 Duct Width	11
2.3 Duct Definition	11
2.4 Duct Frequency Dependence	13
2.5 Propagation Losses For Ducts	13
3. LAYER AND DUCT CHARACTERISTICS	15
3.1 Occurrence of Surface Ducts	15
3.2 Occurrence of Elevated Ducts	16
3.3 Elevated Duct Statistics	19
4. ILLUSTRATIVE EXAMPLES	23
4.1 Application To Broadcasting	27
5. RECOMMENDATIONS	30
6. REFERENCES	32
7. APPENDICES	
A: Ducting Expressions	35
B: Contour Maps For 10 and 90 Percentile Values	38
C: Schematic Representations of Some Meteorological Conditions Favorable For Anomalous Radio Propagation	47
D: List of Symbols	52

LIST OF FIGURES

<u>Figure</u>	<u>Page</u>
1. An atmospheric fading mechanism, Multipath.	3
2. An atmospheric fading mechanism, Isolation.	4
3. An atmospheric fading mechanism, Diffraction.	5
4. Service and interference propagation paths for two systems.	6
5. Elevated layer with a ducting gradient, its refractivity profile, and two trapped radio wave trajectories.	10
6. Elevated layer with a ducting gradient, its modified refractivity profile, and two trapped radio wave trajectories.	10
7. Elevated and surface duct parameters.	12
8. The occurrence of elevated ducts in percent of all hours of the year.	17
9. The occurrence of elevated ducts in percent of all hours of the worst month.	18
10. The locations of the 107 historical radiosonde data stations.	20
11. The median minimum trapping frequency, $f_t(50\%)$ in megahertz.	21
12. The optimum coupling elevation, $h_o(50\%)$ in meters above the surface, expected for 50% of all elevated ducts.	22
13. The median M-unit lapse across the observed elevated ducts, $ \Delta M(50\%) $ in M-units.	24
14. The median base height of elevated ducts, $h_b(50\%)$ in meters above the surface.	25
15. The median elevation of the top of elevated ducts, $h_a(50\%)$ in meters above the surface.	26
B-1. An upper bound for the minimum trapping frequency, $f_t(10\%)$ in megahertz.	39
B-2. A lower bound for the minimum trapping frequency, $f_t(90\%)$ in megahertz.	40
B-3. An upper bound on the base height of the elevated ducts, $h_b(10\%)$ in meters above the surface.	41

<u>Figure</u>		<u>Page</u>
B-4.	A lower bound on the base height of elevated ducts, $h_b(90\%)$ in meters above the surface.	42
B-5.	An upper bound on the optimum coupling elevation, $h_o(10\%)$ in meters above the surface.	43
B-6.	A lower bound on the optimum coupling elevation, $h_o(90\%)$ in meters above the surface.	44
B-7.	An upper bound on the elevation at the top of the ducts, $h_a(10\%)$ in meters above the surface.	45
B-8.	A lower bound on the elevation at the top of the ducts, $h_a(90\%)$ in meters above the surface.	46

LIST OF TABLES

<u>Table</u>		
1.	Comparison of Broadcast Fields in Decibels Below the Free-Space Level at Flint, Mich., for 50% of Receiver Locations 450 to 1000 MHz.	29

LIST OF CHARTS

<u>Chart</u>		
1.	Surface Superrefractive Layers.	48
2.	Surface Subrefractive Layers.	49
3.	Elevated Superrefractive Layers.	50
4.	Elevated Subrefractive Layers.	51

10
11

THE ROLE OF ELEVATED DUCTING FOR RADIO SERVICE AND INTERFERENCE FIELDS

H. T. Dougherty and E. J. Dutton*

This report categorizes the manner in which atmospheric stratification can complicate the problems of frequency allocation and radio regulation by inhibiting service fields and enhancing interference fields. For the United States and its border regions, preliminary contour maps are presented for those parameters associated with the atmospheric layering (ducts) conducive to the propagation of unusually strong UHF and SHF fields over extremely long distances. The parameters of interest are: the percent occurrence of elevated ducts, a minimum trapping frequency, the modified refractivity lapse, the ducting-layer base height, the duct-base height, and the duct-top height. The role of these duct parameters in the prediction of potential interference fields is detailed by engineering formulas and illustrated by numerical examples. These predictions of duct characteristics from historical (radiosonde) data are necessarily preliminary because of present inadequacies of the data sample. Approaches for improving estimates of duct parameters are described. Appendices detail expressions for duct trajectories and map the variation of duct characteristics.

Key Words: anomalous propagation; atmospheric ducts, layers, or stratification; ducting; interference fields; ray trajectories; SHF; UHF

1. INTRODUCTION

Under the influences of climatological and synoptic weather processes such as subsidence, advection, or surface heating and radiative cooling, there is a tendency for the lower atmosphere to stratify. This stratification can take the form of refractivity layering; i.e., layers in which contrasting refractivity gradients occur. Of primary interest here are those layers:

- o with strong ducting gradients ($dN/dh < -157$ N units/km),
 - o immersed within super refractive air ($-157 < dN/dh < -39$ N units/km),
 - or o overlying a sub-refractive layer ($dN/dh > -39$ N units/km);
- the N and h are defined by (2a) and (2b) on page 8. These layers with strong ducting gradients are commonly on the order of ten meters in vertical extent (but often much less), and commonly bounded by layers of localized turbulence. These layers can be horizontally extensive, from tens to hundreds of kilometers in extent, although the thinnest layers may be only kilometers in extent [Dougherty and Hart, 1976; Hall, 1980].

* The authors are with the U. S. Department of Commerce, National Telecommunications and Information Administration, Institute for Telecommunication Sciences, Boulder, CO. 80303.

This atmospheric layering in the troposphere is of concern both to system design engineers and to the national or international radio regulators. Ducting layers have the effect of trapping or guiding (ducting) radio wave energy in their vicinity. On short paths and even line-of-sight (LOS) paths, this ducting may introduce atmospheric multipath or be so efficient as to divert energy away from an intended receiving terminal, depressing the received field level to far below the median service field level (fading). Simultaneously, this efficiently diverted radio energy may be directed well beyond the intended service area to cause an otherwise unexpectedly strong interference signal to other co-channel systems or services.

1.1 Degradation of Service Fields

On line-of-sight (LOS) systems, or over the LOS portions of trans-horizon systems (i.e., between each terminal antenna and its horizon), tropospheric layers can degrade system performance. For example, layers near the surface can:

- (a) introduce additional propagation paths (which constitute atmospheric multipath and produce fading);
- (b) effectively isolate one telecommunications terminal from the other (by diverting the radio wave and attenuating the received signal level);
- or (c) diffract the service propagation path, introducing losses (radio holes) due to the proximity of the radio wave trajectory to media boundaries (such as the earth's surface or the base and top of tropospheric layers).

Examples of each of these categories are illustrated by, respectively, Figures 1, 2, and 3 [Dougherty, 1968].

1.2 Enhancement of Interference Fields

For the avoidance of interference as required by radio regulations [ITU, 1976; NTIA, 1979], the terminals of co-channel systems are normally positioned to avoid an efficient inter-system (interference) propagation path. For the usual trans-horizon potential interference path that then results, the available modes of propagation are volume scattering (troposcatter), diffraction, and (in the presence of tropospheric layers) turbulence-layer scatter, reflection, scatter in the presence of rain, and the strongly refracted (ducted) modes of propagation. Their order in the preceding sentence is that of generally increasing efficiency, but of decreasing availability. Figure 4, illustrates the situation: there, the $T_a R_a$ and $T_b R_b$ dash-dot trajectories represent LOS service paths, isolated from one another by their antenna patterns and the intervening terrain, such as at O. The dashed-line

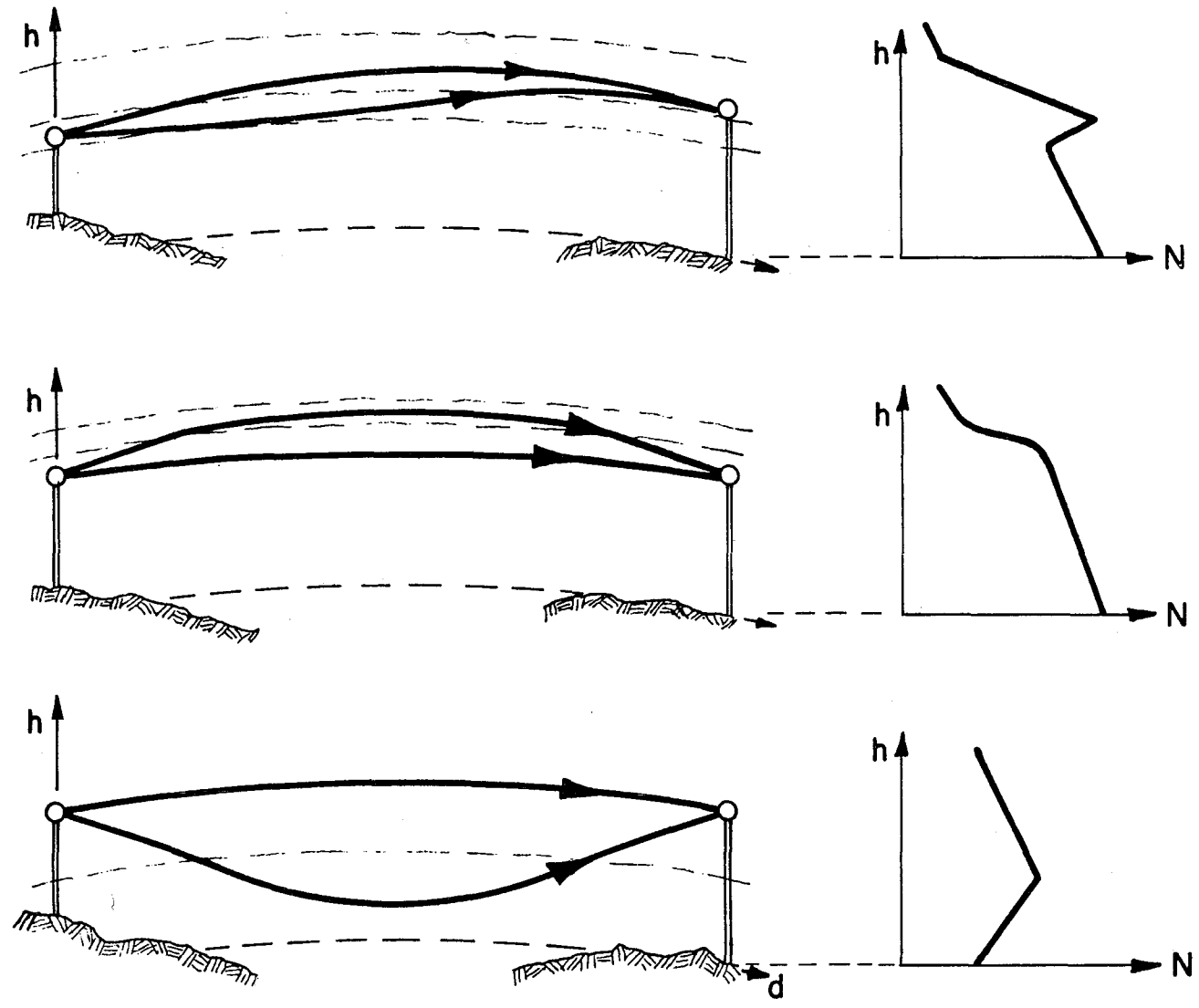


Figure 1. An atmospheric fading mechanism, Multipath [Dougherty, 1968]

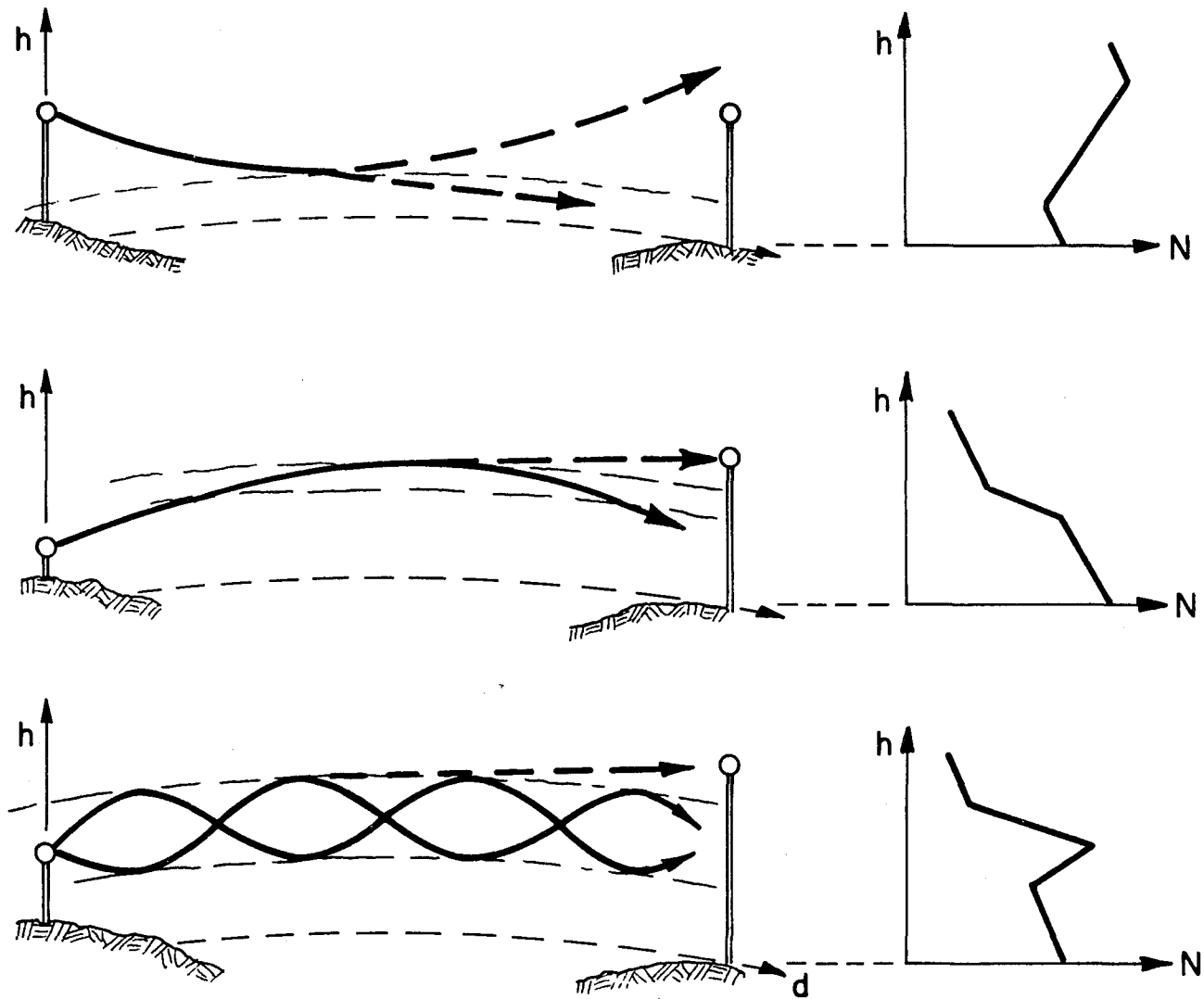


Figure 2. An atmospheric fading mechanism, Isolation. Isolation of terminals, one from another may be caused by atmospheric layers and ducts [Dougherty, 1968].

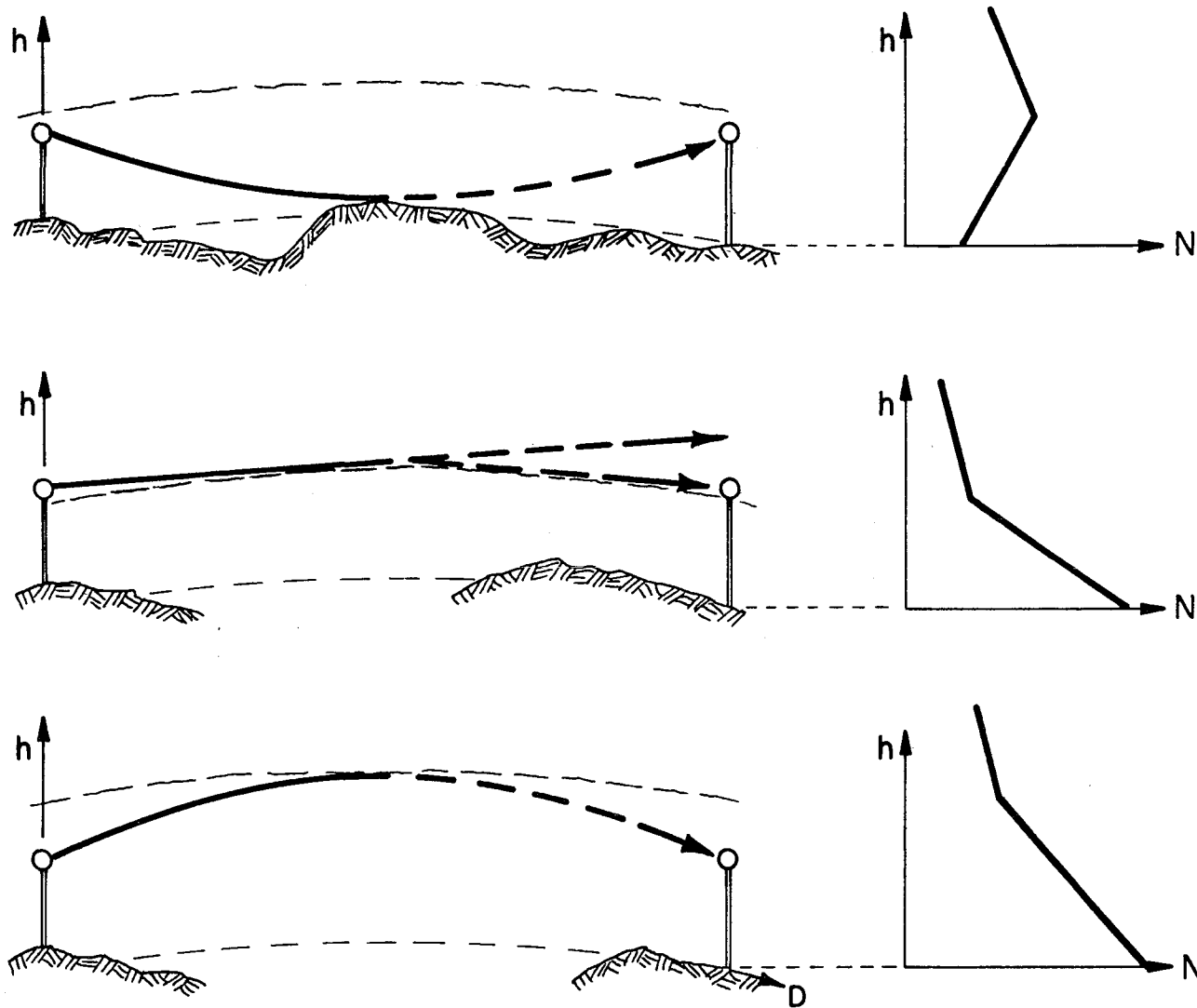


Figure 3. An atmospheric fading mechanism, Diffraction. This loss in a radio hole is encountered whenever the radio wave trajectory approaches too closely to a boundary (such as the earth's surface or the top and base of a layer) [Dougherty, 1968].

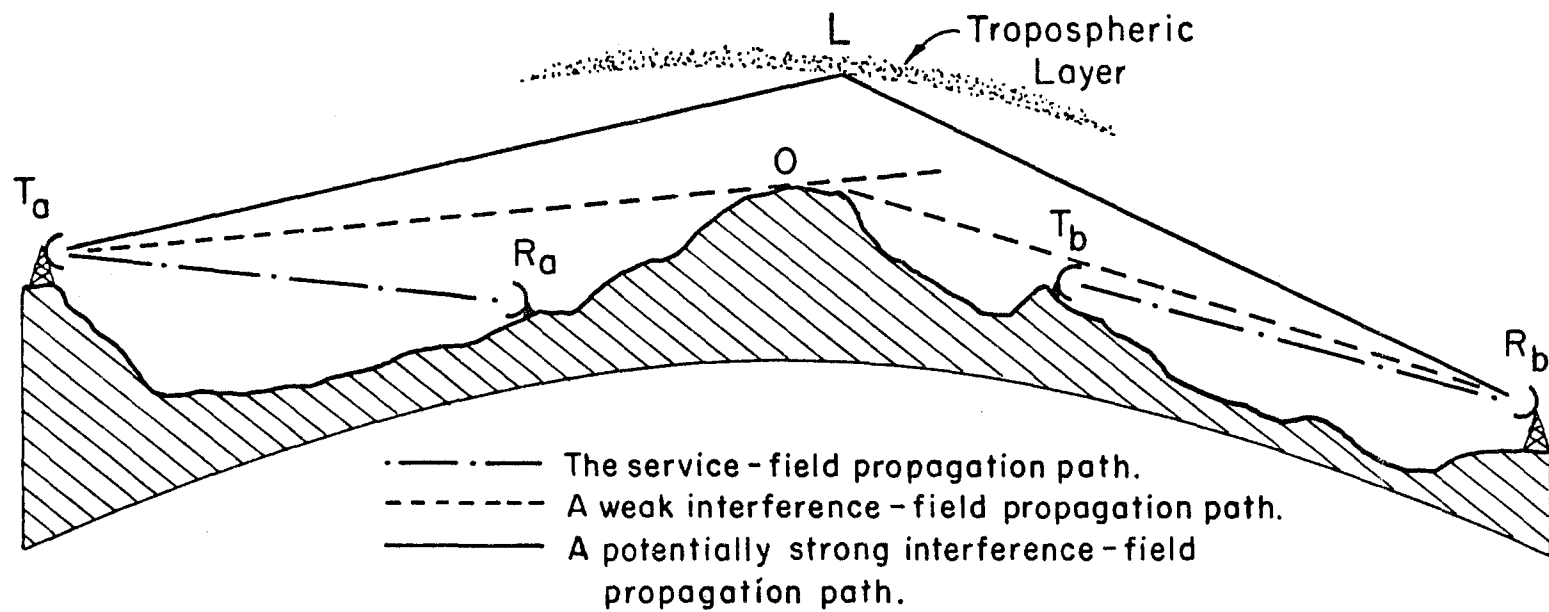


Figure 4. Service and interference propagation paths for two systems.

path T_aOR_b represents a weak (diffracted or troposcatter) interference path [CCIR, 1978a; 1978b], but the continuous-line path T_aLR_b represents a potentially strong interference path, via the ducting layer at L. Of course, additional reflecting layers can provide additional interference path trajectories. Reflection from terrain (between T_a and 0 or R_b and 0) can also provide additional components via the layer at L [Saxton, 1951; Hall, 1968].

Whether a ducting layer causes a radio wave (that is incident upon the layer from below, as in Figure 4) to be scattered, reflected or trapped, depends largely upon the layer's refractivity gradient, the angle of ray incidence measured relative to the layer boundary's tangent, the layer thickness in terms of wavelength and small-scale turbulent fluctuations along the layer boundary. Although detailed descriptions of the relevant parameters are presented in Section 2, we can note here that for critical refraction or ducting by a ducting layer, the grazing angle of incidence from below, θ , must not exceed a critical value θ_c ; i.e., ducting occurs for

$$0 < \theta \leq \theta_c . \quad (1a)$$

For larger angles of incidence, the layer will reflect the incident field with a reflection coefficient given approximately by

$$|\rho| \leq (\theta_c/\theta)^2 / (8\pi\delta \sin \theta) \ll 1.0, \quad \theta > \theta_c . \quad (1b)$$

Here, δ is the layer thickness expressed as a multiple of the radio wavelength [Wait, 1964, 1969; Dougherty and Hart, 1976; Hall, 1980]. For a given layer, δ will increase with decreasing wavelength so that the above equation indicates a reflection coefficient that tends to decrease with increasing radio wave frequency. For this reason, layer reflection would be expected to play the more important role in interference at VHF and for paths up to a hundred kilometers or so in length, but become of decreasing importance for increasing radio frequency at UHF and for very long paths. On the other hand, the strong refraction of radio waves by these layers (ducting) tends to become increasingly important at UHF and higher frequencies and particularly for long paths.

The thin turbulent layer that commonly bounds the refractivity gradient layer will also provide a backscatter signal. This has been used as the basis for monitoring the occurrence and motion of tropospheric layers [Bean et al., 1971; Dougherty and Hartman, 1977; Crane, 1980].

2. DUCTING STRUCTURES

Among the broad array of features which characterize atmospheric layers, specific parameters have been defined that have a particular relevance for radio wave propagation. The most prominent of these would be the radio refractive index structure or its equivalent. For example, the bending of a radio wave's trajectory through the atmosphere results primarily from the spatial variation of the atmospheric refractive index $n(h)$ with elevation h above the surface. However, a more sensitive measure of this $n(h)$ structure is given by the refractivity structure $N(h)$:

$$N(h) = [n(h) - 1] 10^6 \quad \text{N units,} \quad (2a)$$

and its vertical gradient

$$\frac{dN}{dh} = 10^6 \frac{dn}{dh}, \quad \text{N units/km.} \quad (2b)$$

Nevertheless, in describing the effects of this structure upon radio propagation, it is often more convenient to describe the gradient in terms of the modified refractivity structure $M(h)$,

$$M(h) = N(h) + 157h \quad \text{M units,} \quad (2c)$$

and its gradient

$$\frac{dM}{dh} = \frac{dN}{dh} + 157 \quad \text{M units/km.} \quad (2d)$$

This modified refractivity results from the geometrical transformation from a spherically stratified atmosphere above a spherical path to a planar stratification above a flattened earth. This is described in Appendix A and will be illustrated in the next section. For an elevated ducting layer ($dM/dh < 0$ M units/km), the critical angle of incidence (upon the layer from below) mentioned in (1a) is given by

$$\theta_c = \sqrt{2|\delta M|} \quad \text{mrad,} \quad (3a)$$

i.e., in milliradians [Gough, 1962]. Here the M-lapse δM is determined from

$$\delta M = \frac{dM}{dh} \cdot \delta h \cdot 10^{-3} \quad \text{M units,} \quad (3b)$$

for a layer thickness δh in meters and the gradient dM/dh in M units/km. There is,

of course, a corresponding negative critical angle of incidence (upon a layer from above) when the layer gradient of modified refractivity is positive ($dM/dh > 0$ M units/km). Its magnitude is still determined from (3a) and (3b). The value given by (3a) is at the layer base h_0 .

2.1 Ducting

For those angles of incidence at the layer base that are equal to or less than the critical value of (3a), the incident wave from below is refracted (bent) by a trapping layer of ($dM/dh < 0$ M units/km) and may propagate efficiently (be ducted) for long distances. This is illustrated by Figure 5. To the left of Figure 5, the vertical refractivity profile $N(h)$ depicts a layer δh meters thick with a gradient $(dN/dh)_0 < -157 N$ units/km and at a base height of h_0 meters above ground. Above and below the layer, there are standard gradients ($dN/dh \approx -39 N$ units/km). The remainder of Figure 5 depicts the layer extending over an effective earth curvature R_e that is $4/3$ that of the true earth, i.e., $R_e = 4/3 R_0$, $R_0 = 6370$ km. In this situation, a radio wave launched at the layer base height h_0 at (or less than) the critical angle will follow a curved path (as illustrated, from $0''$ to a to 0 or $0''$ to a' to $0'$) within the layer. A radio wave traveling exterior to the layer will follow a straight path.

Consider a wave trajectory (ray path) launched from point $0''$ in Figure 5 at an initial elevation angle $\theta_0 < \theta_c$. Its dashed-line trajectory is strongly refracted so that, after achieving a maximum elevation at a' , it returns to the layer base at $0'$. It continues, emerging from the layer at an elevation angle $\theta = -\theta_0$, relative to the layer tangent at $0'$, to travel in a straight-line trajectory past an elevation minimum at b' to again intercept the layer at its base. There is, of course, a maximum launch angle $\hat{\theta}_0$ at $0''$ that will restrict the trajectory elevation to a maximum coinciding with the layer top at point a . The continuous-line trajectory of Figure 5 illustrates this launch angle $\theta = \hat{\theta}_0$. The minimum elevation of the trajectory occurs on the straight-line at b as the trajectory continues to a re-entry of the layer. The value of $\hat{\theta}_0$ is given by (3a), i.e., $\hat{\theta}_0 = \theta_c$.

These two elevation extremes, $h_a = h_0 + \delta h$ at the top of the ducting layer and h_b well below the base of the layer, constitute the bounds on wave trajectories for trapped radio waves. The duct width or thickness D exceeds the thickness of the layer δh ,

$$D = h_a - h_b = \delta h + [h_0 - h_b] \quad (4)$$

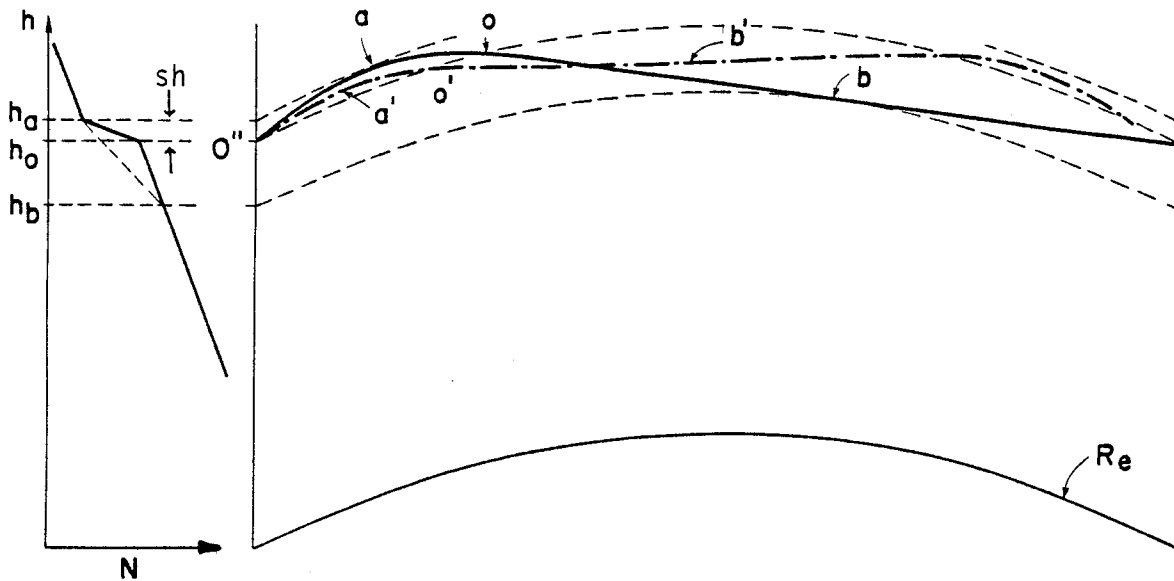


Figure 5. Elevated layer with a ducting gradient, its refractivity profile, and two trapped trajectories. The reference elevation is for an effective earth radius R_e .

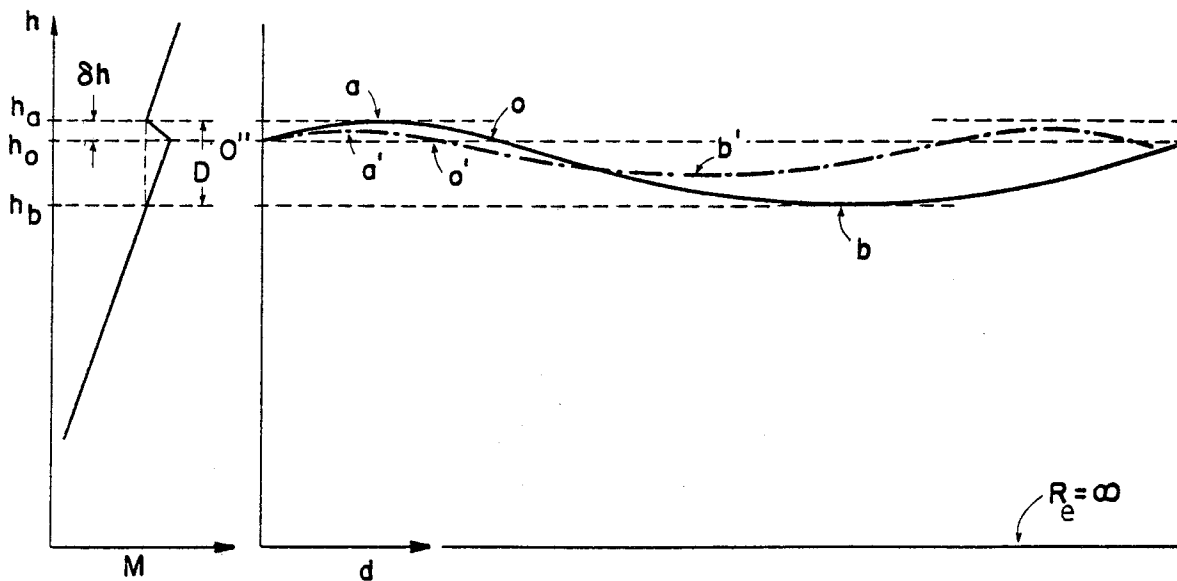


Figure 6. Elevated layer with a ducting gradient, its modified refractivity profile, and two trapped trajectories. The reference elevation is for a flattened earth. D is the duct thickness; δh is the layer thickness.

The trajectories of Figure 5 have been called earth-detached ducting modes (Wait, 1962).

2.2 Duct Width

Figure 6 is a replotting of Figure 5 for the flattened earth. The modified refractivity profile $M(h)$ is shown at the left. Note that the top of the duct at h_a and the bottom of the duct at h_b have the same M value,

$$M(h_a) = M(h_b) \quad (5)$$

The remainder of Figure 6 illustrates the conventional symmetrical trajectories associated with duct propagation. The trajectories are well approximated as parabolic within a layer of constant gradient [Millington, 1957; Dougherty and Hart, 1979]. See Appendix A.

From (3b), (4), and (5), the duct width is given by

$$D = \delta h \left[1 - \left\{ \left(\frac{dM}{dh} \right)_o / \left(\frac{dM}{dh} \right)_b \right\} \right] \quad (6)$$

where $(dM/dh)_o$ is the (negative) modified refractivity gradient across the ducting layer and $(dM/dh)_b$ is the (positive) modified refractivity gradient below the ducting layer.

2.3 Duct Definitions

In addition to the trajectories illustrated in Figure 6 with positive launch angles, there is also an array of trajectories that could be launched at 0° for negative angles $\theta > -|\theta_c|$. Inspection of Figures 5 and 6 should make it clear that any trapped wave trajectory will cross the duct axis (the optimum elevation h_o) at an angle whose magnitude has the limit $|\theta| \leq |\theta_c|$ relative to the layer tangent at that point. For the situation illustrated in Figures 5 and 6 where $h_b \geq 0$, a trapped trajectory continues as earth-detached. If the ducting layer were lowered ($h_b \leq 0$) and if the earth's surface were sufficiently smooth, a trapped trajectory could strike and be reflected from the surface. Then the lower boundary of the duct would be provided by the smooth surface; the duct would be a ground-based duct, although the layer would still be elevated ($h_o > 0$). Duct propagation then would involve both earth-detached and earth reflected trajectories.

Figure 7 illustrates the three categories of ducts. Note that a ground-based layer ($h_o = 0$) will also constitute a ground-based duct; then, the layer thickness δh equals the duct thickness D and ground reflection is essential to duct propagation.

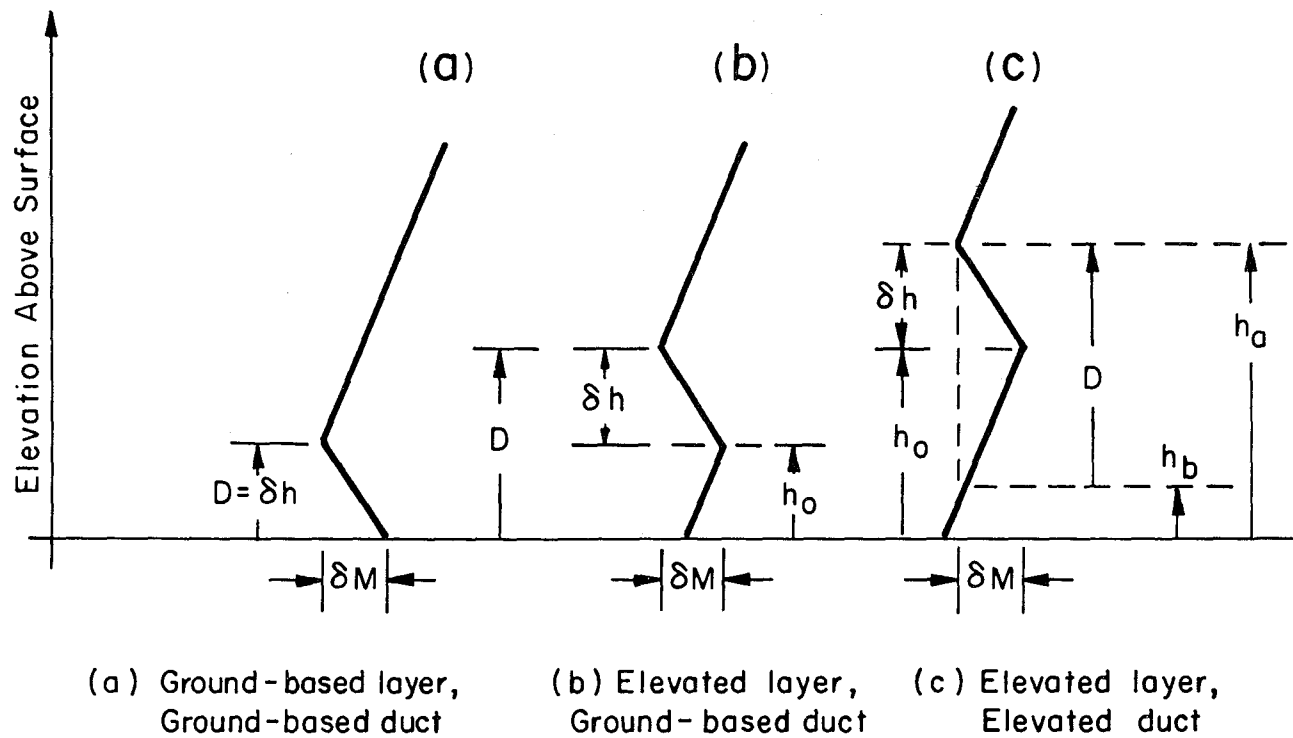


Figure 7. Elevated and surface duct parameters.

If the reflecting surface has a slope, the additional tilt imparted to the reflected trajectory may permit it to escape the duct.

2.4 Duct Frequency Dependence

Early work in duct propagation defined a minimum (cut-off) frequency of propagation by an analogy to waveguide transmission [Kerr, 1951]. However, experimental studies have demonstrated that the "cut-off" effect occurs over a range of frequencies rather than abruptly at a specific frequency. The Wait and Spies (1969) full-wave solution of duct propagation showed that propagation normally occurs with very low losses for earth-detached modes. However, the loss coefficient, α in dB/km of path length, increases rapidly for decreasing frequencies approaching a critical value. A.S. Ratner (private communications) showed that for frequencies greater than trapping value

$$f_t = \frac{1572}{D^{1.8}} \text{ GHz} \quad (7)$$

radio energy will propagate with a loss coefficient $\alpha < 0.03$ dB/km. For lower frequencies, the coefficient would be expected to increase rapidly [Neesen and deHaas, 1980]. In (7), the duct thickness D is in meters.

2.5 Propagation Losses for Ducts

Propagation within a duct has long been the subject of theoretical as well as experimental investigation; evaluation of propagation losses dates to Kerr [1951]. Wait has placed the very wide variety of solutions into a common context [Wait, 1962]; they all assume horizontally uniform ducts (ducts whose characteristics, h_0 , D , f_t , etc., do not vary horizontally). Since, the full-wave solutions have been extended to piecewise uniform ducts, a significantly closer approach to atmospheric ducts [Bahar and Wait, 1965; Cho and Wait, 1978]. Currently there are widespread efforts to relate the full-wave modal solutions for duct propagation to the ray-trajectory formulation [Cho et al., 1979; Migliora et al., 1980; Ott, 1980]. This could provide the advantage of leading to engineering-type solutions. For the present, however, there are empirical bounds that can be given for the role of duct propagation in interference fields [Dougherty and Hart, 1979].

Commonly for tropospheric radio wave propagation, the free-space field or the free-space basic transmission loss is taken as a reference. That assumes an inverse-square dependence upon the propagation path length, since the field expands in the two dimensions normal to the direction of propagation. However, in duct propagation, because of the trapping constraint on spreading in one (vertical)

dimension, the reference loss within the duct will have only an inverse-distance dependence on distance. However, there is still the loss, $\alpha \leq 0.03$ dB/km. For propagation between two terminals within a duct, i.e., when both terminals are immersed within the duct, the basic transmission loss is

$$L_b \geq 92.45 + 20 \log f + 10 \log d_0 + \alpha d_0 + \sum A \text{ dB}, \quad (8)$$

for the frequency $f > f_t$, in gigahertz and the path length within the duct, d_0 in kilometers. For the earth-detached modes illustrated by the wave trajectories of Figures 5 and 6, $\alpha \leq 0.03$ dB/km; for the $h_b \leq 0$ and ground-reflected modes, the appropriate α would be much larger [CCIR, 1978c]. The summation term in (8) is the sum of coupling losses discussed below. Note that the first three terms of (8) differ from the expression for the free-space basic transmission loss

$$L_{bo} = 92.45 + 20 \log f + 20 \log d \text{ dB}. \quad (9)$$

only in the coefficient 10 rather than 20 for the third term. For f in megahertz, the first term in (8) and (9) would be the familiar 32.45 [CCIR, 1978d].

For an actual telecommunications system with non-isotropic antennas, the minimum transmission loss would be given by (8) minus the antenna power gains in decibels above an isotropic dBi). Since only that energy would be trapped that lies within the range $-\theta_c \leq \theta \leq \theta_c$, there is for each terminal an antenna-media coupling loss

$$\begin{aligned} A_c &= -10 \log (2|\theta_c|/\Omega) \text{ dB}, & 2|\theta_c| < \Omega, \\ &= 0.0 \text{ dB} & , \quad 2|\theta_c| > \Omega, \end{aligned} \quad (10)$$

for an antenna lobe's half-power beamwidth of Ω in milliradians directed along the duct.

When the terminal antenna's center of radiation is at h_0 (the optimum coupling elevation), θ_c is given by (3a); at other elevations, see Appendix A. There is a similar coupling loss when the antenna's center of radiation is within the same elevation range of the duct but just beyond the duct's horizontal extent. Then the θ_c of (10) would be replaced by D/d_L where D is the duct width of (6) and d_L is the distance from the end of the duct to the terminal beyond (exterior to) the duct. When an antenna is external to and above or below the duct, the antenna-media coupling loss of (10) is replaced by

- a), a basic transmission loss given by (9) for that portion of the path length that is exterior to the duct,

plus b), an interior/exterior coupling loss of about 6 dB when the terminal is above the duct and about 10 dB or more when the terminal is below the duct [Dougherty and Hart, 1979].

In order for a wave trajectory drawn from a point below a duct to be trapped within a horizontally uniform duct, the trajectory must have a grazing incidence from below at the duct base elevation h_b . Therefore, unless the elevated duct is bounded below by another ducting layer, it appears that trapping of a wave trajectory (from below the duct) would require either a discontinuity in the duct or a tilt in the duct base; a wavy structure is a feature not uncommon in elevated ducts [Gossard, 1962; Gossard and Richter, 1970; Bean et al., 1971]. A recent experimental study observed that efficient coupling into (and out of) an elevated duct was associated with an unspecified periodicity in the duct structure [Crane, 1980]. A later section will apply the foregoing expressions in a specific example.

There are additional losses in duct propagation attributable to discontinuities in the duct structure and to other atmospheric conditions, such as the frequency-and-time-dependent absorption by the gaseous atmosphere [CCIR, 1978e; 1978f].

3. LAYER AND DUCT CHARACTERISTICS

In the case of layer-reflected modes and ducted modes of propagation, either as inhibitors of service fields or as enhancers of interference fields, the basic requirement is the presence of tropospheric layers of sufficiently strong (i.e., ducting) gradients. Given their presence, the efficiency of propagation associated with these layers is determined by their positioning (h_b, h_o, h_a) relative to the telecommunication terminals and their trapping frequency relative to the telecommunication system's transmission frequency.

3.1 Occurrence of Surface Ducts

The occurrence of refractivity gradients averaged over the first 100 meters above the surface has been described from historical meteorological data on a worldwide basis [Bean et al., 1966]. More recently, additional data have become available for selected areas, notably the northern hemisphere [Samson, 1975], Canada [Segal and Barrington, 1977], and India [Majumdar et al., 1977]. From these data, we can take the occurrence of initial gradients ($dN/dh < -157$ N units/km) as direct measures of the occurrence of ground-based ducts that are 100 meters thick. Of course, the dependence upon surface reflections (and increased propagation loss) in such ducts will not be clear, since the strong ducting gradient may have occurred either at the surface or slightly elevated within that initial 100 meters. On overwater paths, the distinction has usually been maintained; some ocean areas have been extensively mapped for the probability of long-distance propagation via shallow evaporation ducts

or via the deeper advection ducts with slightly elevated layers [Dougherty and Hart, 1976].

There are some uncertainties associated with these ground-based ducts, especially those observed at the many recording stations on land. The widespread simultaneous observation of ducts over land does not mean, necessarily, that these ducts are horizontally extensive (i.e., continuous) unless the terrain is approximately flat. The larger-scale irregularities of terrain (hills, cities, etc.) tend to modify the characteristics and limit the continuity or horizontal extent of ducts over land. Sea-surface ducts tend to be more prevalent and extensive than those over land, although there is some evidence that ocean depth and ocean currents can limit their horizontal extent. Nevertheless, although individual ducts are of finite length, there is little physical justification for an abrupt specific limit to horizontal duct dimensions. The limit has to be statistically defined, perhaps also varying with climatology and geographical locations, for which there are inadequate data at present for the limits of either overland or oversea surface ducts.

3.2 Occurrence of Elevated Ducts

Descriptions of elevated layer statistics are also available worldwide [Bean et al., 1966; Cahoon and Riggs, 1964] and for selected locales [Dougherty et al., 1967; Hall and Comer, 1969; Segal and Barrington, 1977; Ortenburger et al., private communication]. These provide annual and/or worst-month summaries for the occurrence of ducting and/or superrefractive elevated layers and/or their associated elevated duct parameters (dN/dh , δM , δh , h_b , h_o , D , f_t , etc.), all based upon historical radiosonde data. Figure 8 is a contour map for the United States, of the occurrence of elevated ducts as a percent of an average year, but based on only five years of radiosonde data. Except for the California Coast, the higher values of percent occurrence of elevated ducts (i.e., elevated layers with ducting gradients) is more common in the eastern half of the United States.

Figure 9 is a similar presentation except the occurrence is the percent of the worst months. The worst month is the month with the highest occurrences of elevated ducts. For most of the Nation, the worst month occurs in the summer, midsummer in West, late summer in the East. Along the Gulf Coast, the worst month occurs in the Spring. There are exceptions to these broad generalities. The worst month occurs in the Fall in the great basin (centered on Nevada and the desert portions of California, Arizona, and Utah) and in northwest Florida and the southern portions of Georgia, Alabama, and South Carolina.

Since these data are deduced from radiosonde measurements of the vertical structures of atmospheric temperature and humidity, they carry some limitations not appli-

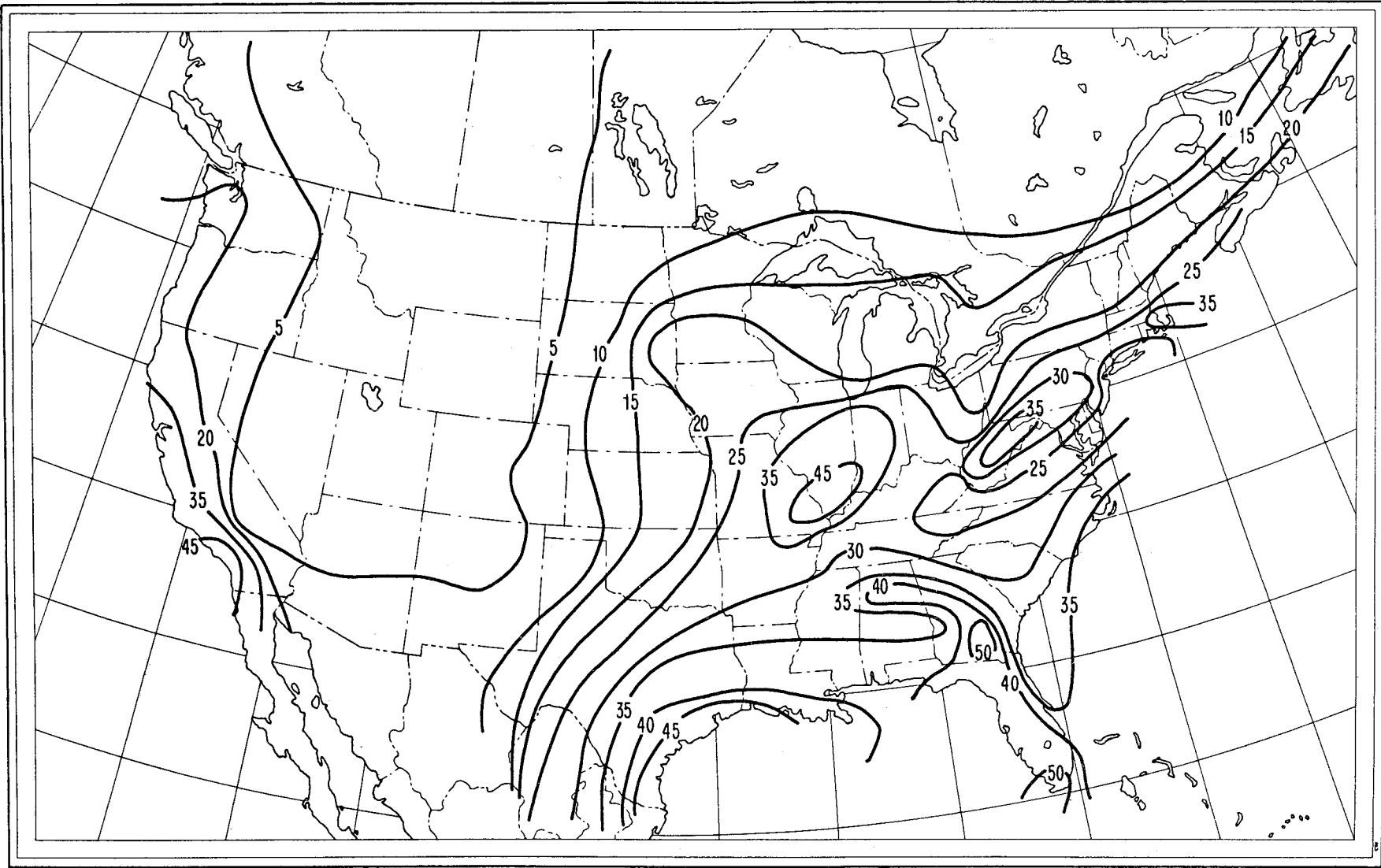


Figure 8. The occurrence of elevated ducts in percent of all hours of the year.

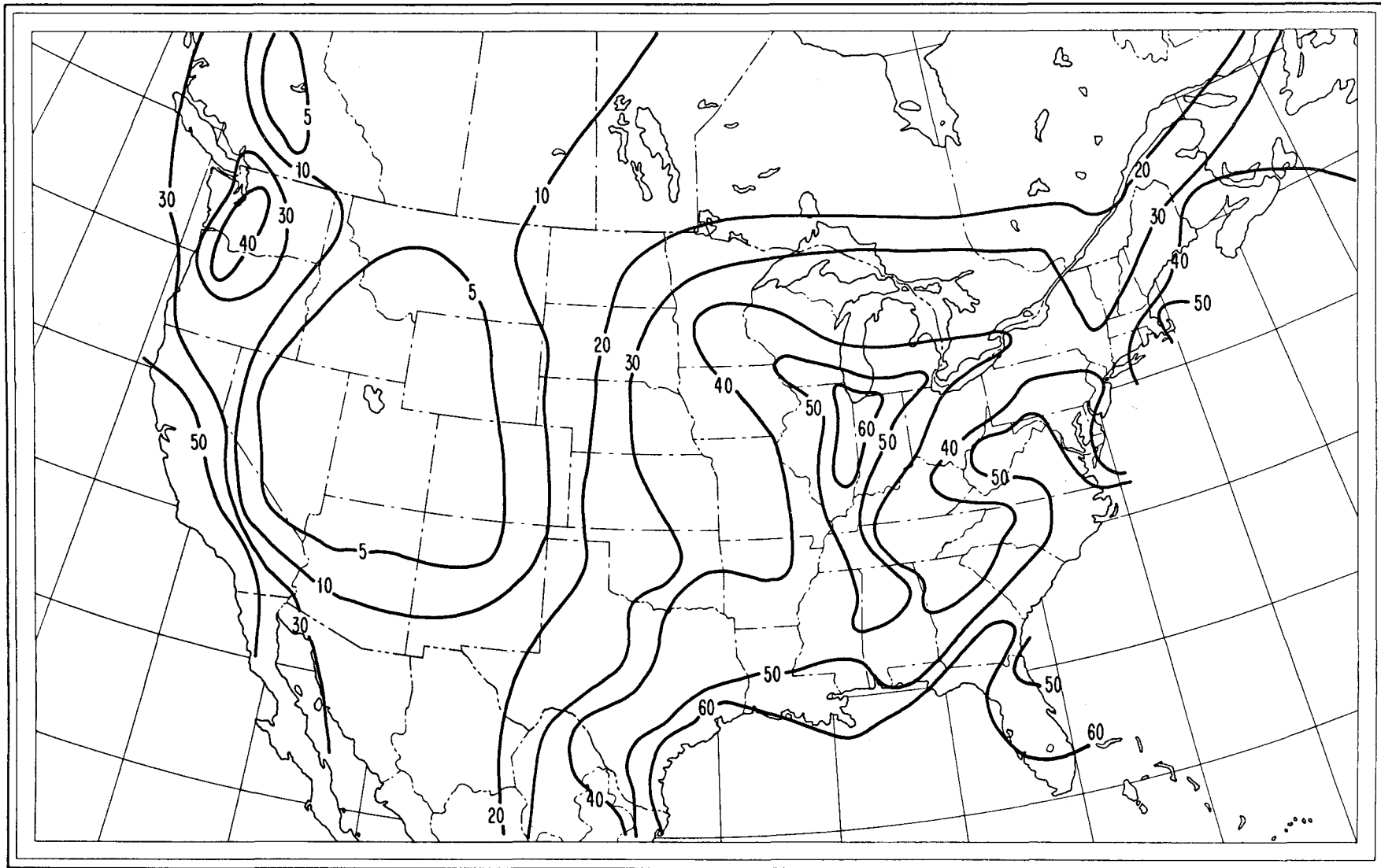


Figure 9. The occurrence of elevated ducts in percent of all hours of the worst month. For no month of the year would the expected occurrence of elevated ducts exceed the indicated values.

cable to the raw data. For example, the radio meteorologist is concerned with the vertical refractivity structure on a much finer scale than is of interest to the (non-radio-) meteorologist who collects the data. The radiosonde instruments' sensor response times and their sequential measure of temperature and humidity, although adequate for the National Weather Service's interests, do cause an overestimation of the elevated layer's thickness and an underestimation of its refractivity gradients [Bean and Cahoon, 1961; Bean and Dutton, 1961]. Since a gradient $dN/dh < -157$ N units/km is evidence of an elevated duct, systematic underestimation means that ducting gradients occur somewhat more frequently than would be deduced from the data. Crane (1980) reported that the observation of ducts by radar surveillance was more frequent than indicated by radiosonde data. Similarly, the transition frequency, deduced through (7) from estimates of D in (6), is somewhat erroneous because of overestimates of δh and underestimates of $(dN/dh)_0$.

There is another disadvantage of estimating the occurrence of elevated ducts from historical meteorological data. Radiosonde data are usually collected twice a day (at 1200 and 2400 GMT) which may or may not correspond to the most favorable time of the day for the occurrence of ducts at each location. The data may, therefore, either overestimate or underestimate the day-by-day occurrence of ducts. Despite these disadvantages, their corrections could be estimated from additional effort and data so that the large body of historical data would still be useful. For example, identification of the sensor types will permit a correction in the estimates of the layer gradient and thickness [Dougherty et al., 1967]. Correlation of radiosonde historical data at certain locations with direct refractometer data obtained nearby [Bean, 1979] would permit estimated corrections for the occurrence of layers and some of their spatial variation.

3.3 Elevated Duct Statistics

Figure 10 locates the 107 radiosonde stations in the contiguous United States and nearby portions of Mexico and Canada that constituted the sources of the five-year data base for the elevated duct statistics [Ortenburger et al., private communication].

Figure 11 is a contour map of the median minimum trapping frequency, $f_t(50\%)$, for the elevated ducts. This was based upon (7) and the median duct thickness data, $D(50\%)$. Although the $f_t(50\%)$ values are usually UHF, they are in the upper VHF range along the Gulf coasts and coasts of southern California and Florida. Of course, the duct thicknesses vary; the range of the resulting f_t values is indicated by the additional contour maps of $f_t(10\%)$ and $f_t(90\%)$ in Appendix B.

Figure 12 is a contour mapping of the optimum coupling elevation expected for 50% of elevated ducts. For example, the optimum coupling elevation (i.e., the

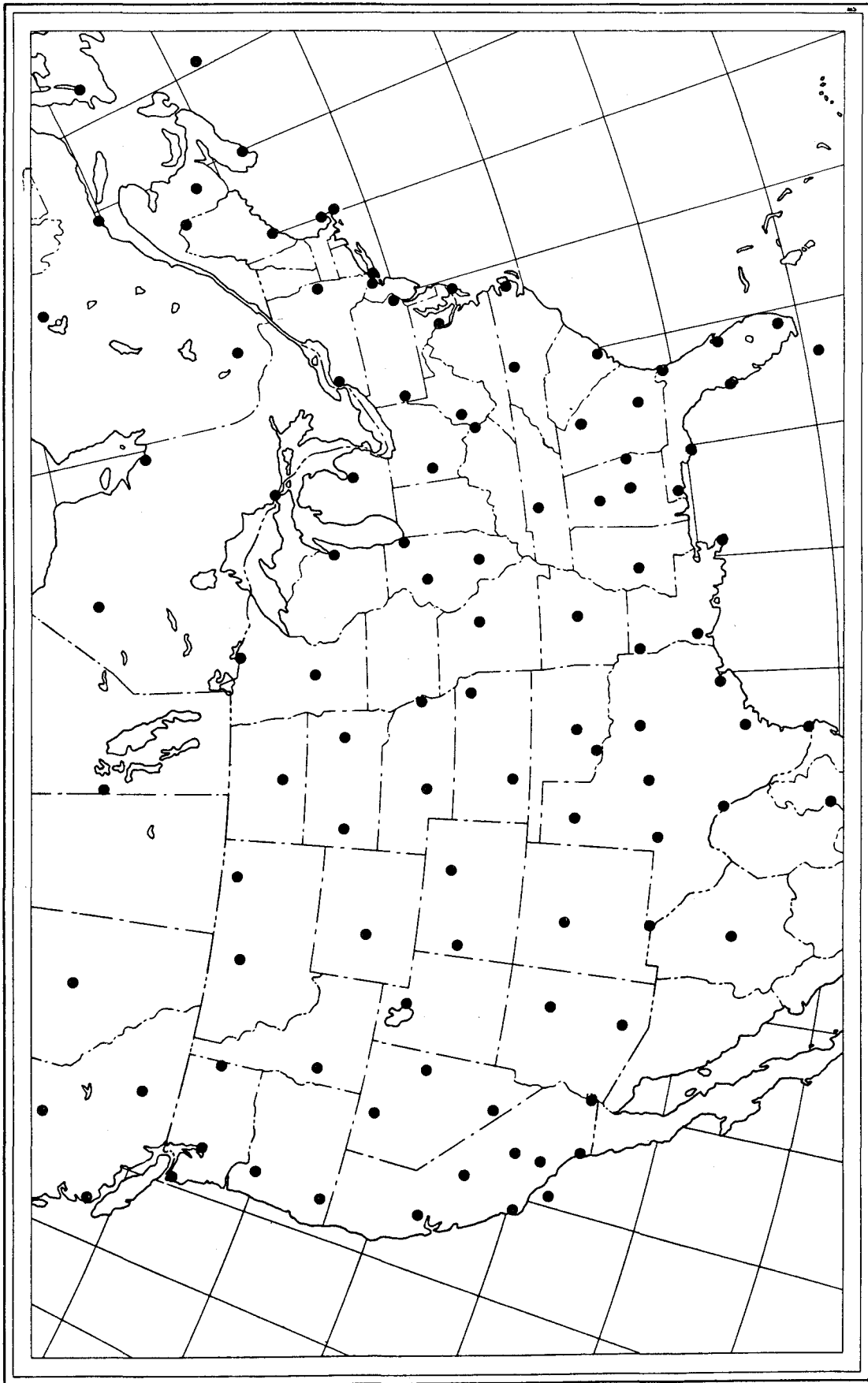


Figure 10. The locations of the 107 historical radiosonde data stations.

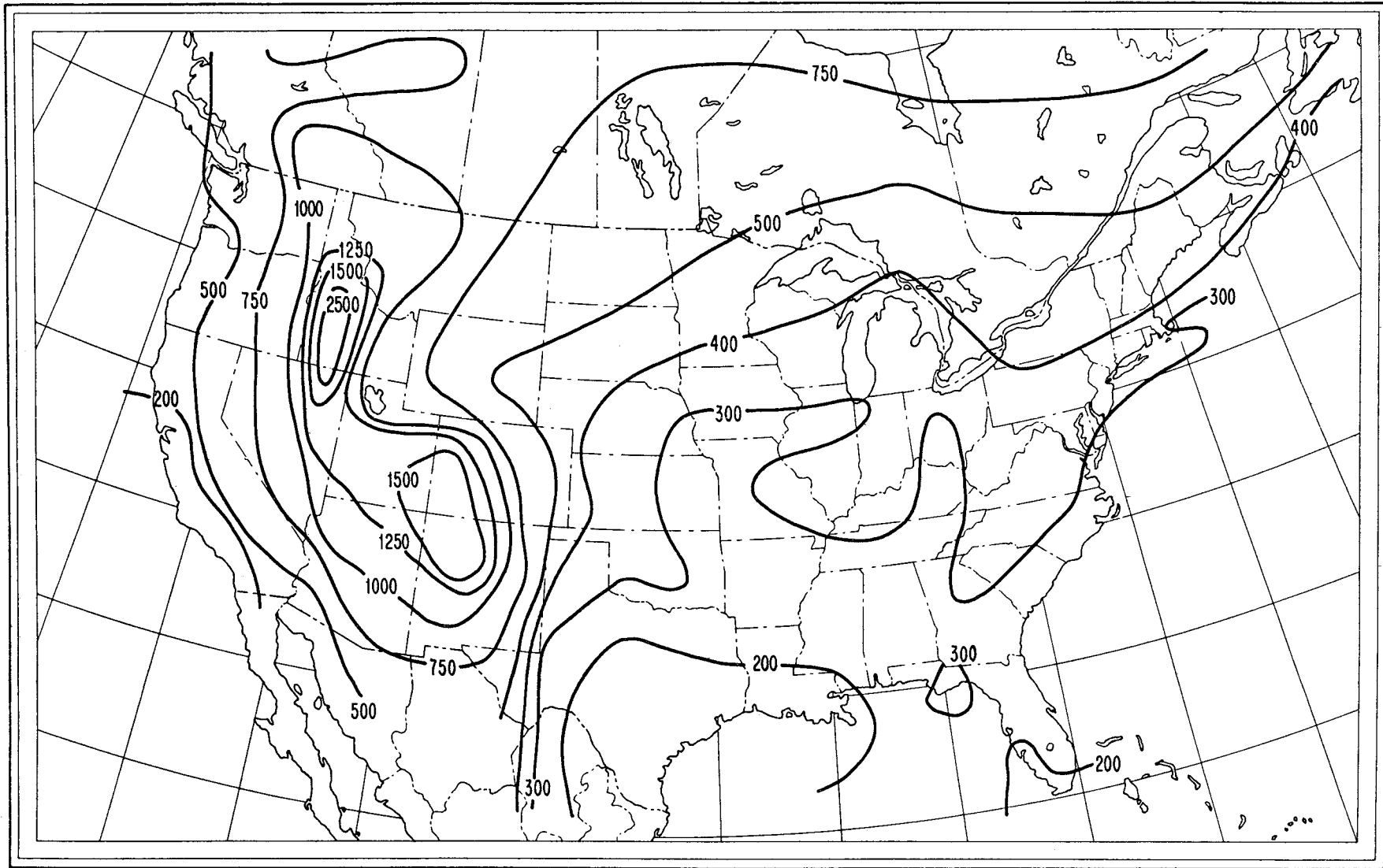


Figure 11. The median minimum trapping frequency, $f_t(50\%)$ in megahertz.

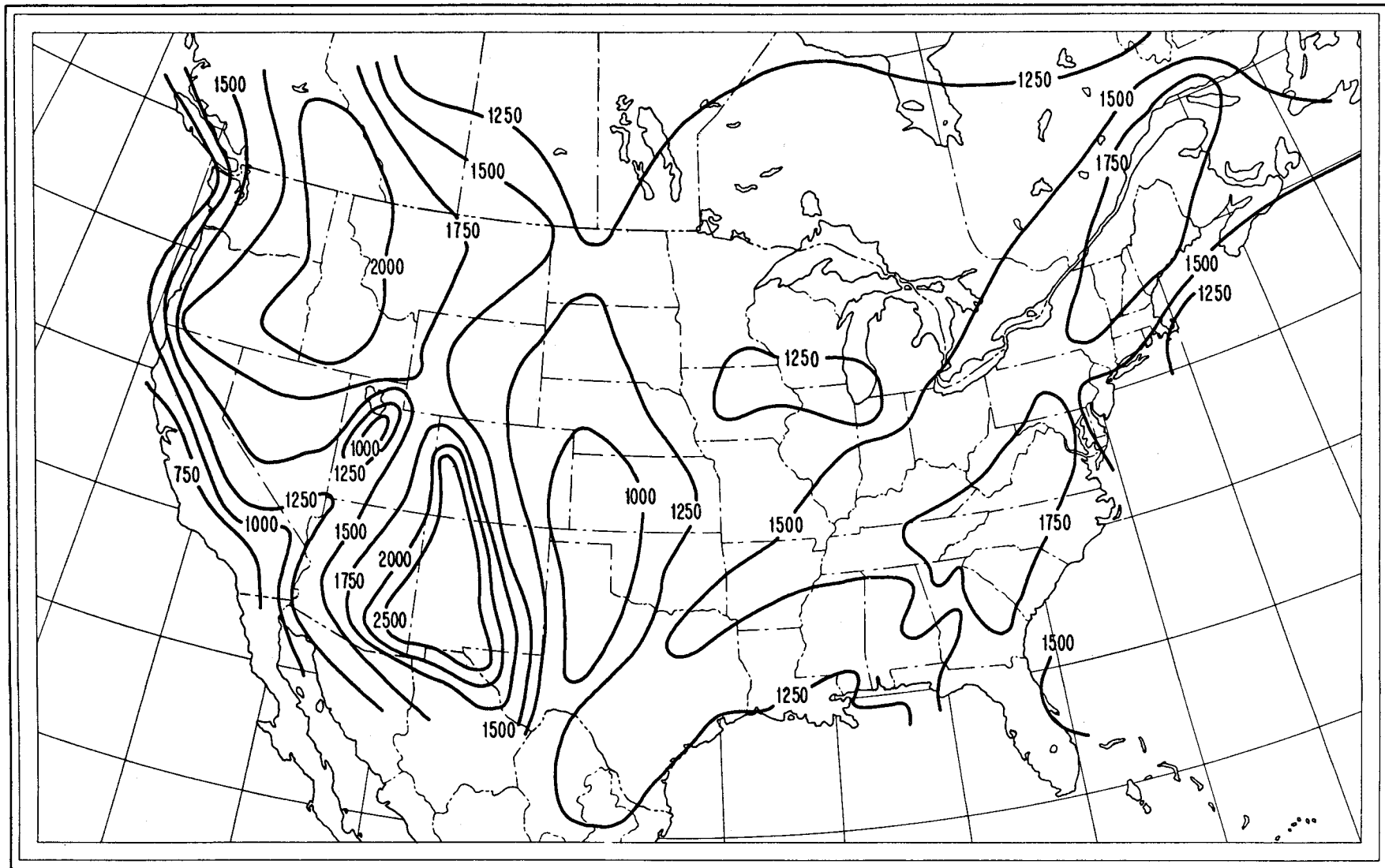


Figure 12. The optimum coupling elevation, $h_0(50\%)$ in meters above the surface, expected for 50% of all elevated ducts.

layer base elevation and the optimum elevation for launching or receiving energy in the duct) over the lower half of Lake Michigan is $h_o = 1250$ meters above the surface.

The median M-unit lapse, $|\Delta M(50\%)|$, of all elevated ducts is given by the contour mapping of Figure 13. Over the southern half of Lake Michigan $|\Delta M(50\%)| \approx 4$ M-units, so that the median critical ducting angle expected at the optimum coupling elevation h_o is, from (3a), $\theta_c(50\%) \approx \sqrt{8}$ milliradians.

In Figures 14 and 15, contour mappings are presented for the median elevations of the base and top of elevated ducts, respectively, $h_b(50\%)$ and $h_a(50\%)$ in meters above the surface. Over the southern portion of Lake Michigan, for example, the median duct base $h_b(50\%)$ is at about 1200 meters and the median duct top $h_a(50\%)$ is at about 1700 meters above the surface.

Of course, each of the foregoing parameters (h_b, h_o, h_a, f_t) can vary from duct to duct; however, an estimate of the range of their values may be deduced from the 10 and 90 percentile values. These are given by the contour maps of Appendix B.

4. ILLUSTRATIVE EXAMPLES

To illustrate the use of the foregoing material in the estimation of expected interference fields, consider the Great Lakes region of the United States. That region is characterized by warm humid summers and cold cloudy winters; atmospheric layering is somewhat more prevalent in the summers.

From Bean et al. (1966), at Flint, Michigan, between Lakes Huron and Erie (one of the stations in Figure 10), surface ducts occur about 2% of the time both in August and as averaged over the four seasons with a median thickness of $D(50\%) \approx 100$ m. The corresponding minimum trapping frequency is, from (7),

$$f_t(50\%) = \frac{1572}{(100)^{1.8}} = 0.39 \text{ GHz} . \quad (11a)$$

That is, frequencies above about 400 MHz will be trapped by surface ducts for about $p = 0.5(2\%) = 1\%$ of the time. This observation of surface ducts is actually the observation of refractivity gradients < -157 N units/km, "over the initial 100 m above the surface (i.e., a change of at least 15.7 N units). From an examination of Figure 7, this refractivity lapse could have been provided by a variety of structures. If we assume it is entirely due to an elevated layer of thickness $\delta h = 10$ m, then

$$\frac{dN}{dh} \leq - \frac{15.7}{10} = -1.57 \text{ N units/m} = -1570 \text{ N units/km} . \quad (11b)$$

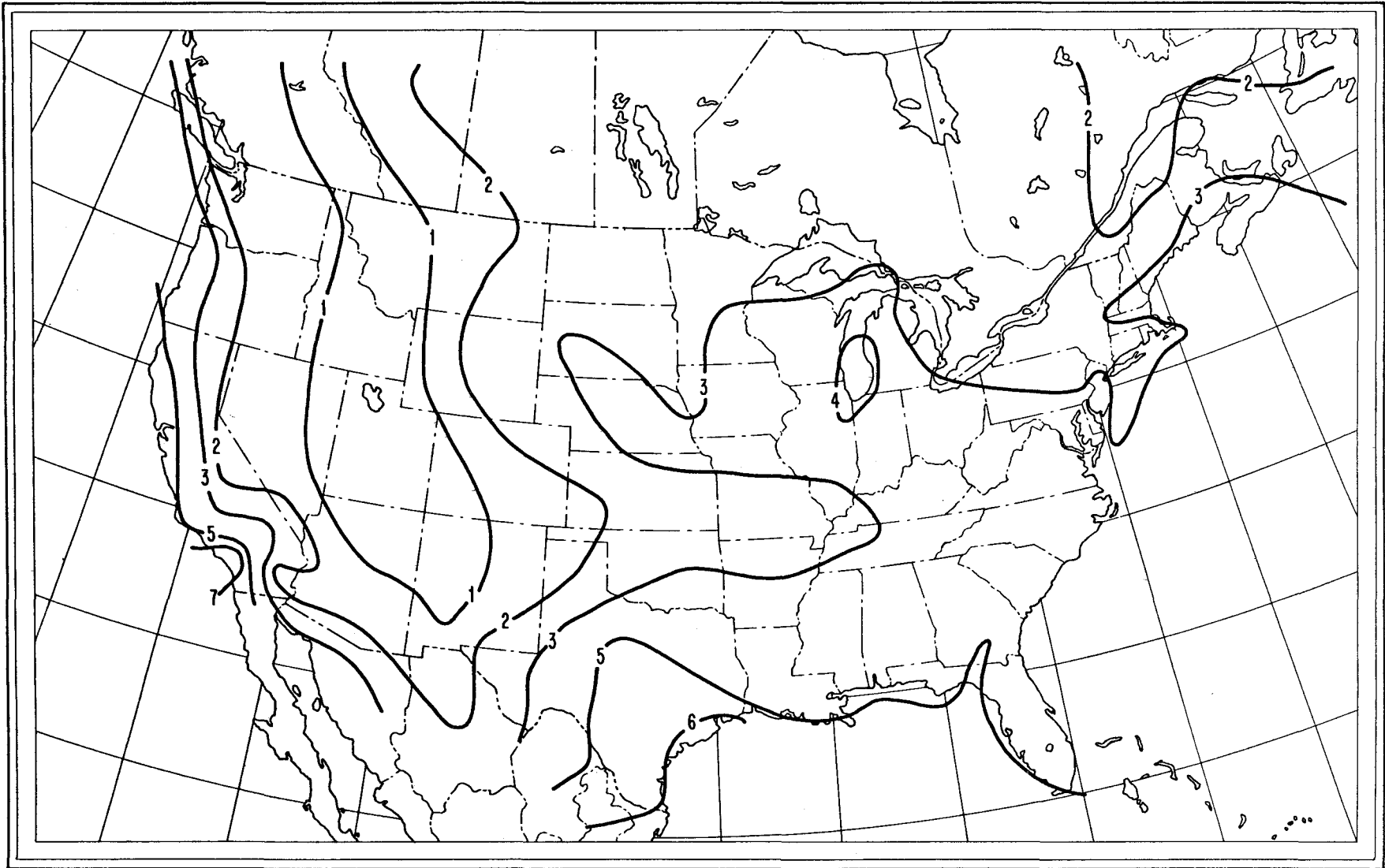


Figure 13. The median M-unit lapse across the observed elevated ducts, $|\Delta M(50\%)|$ in M-units.

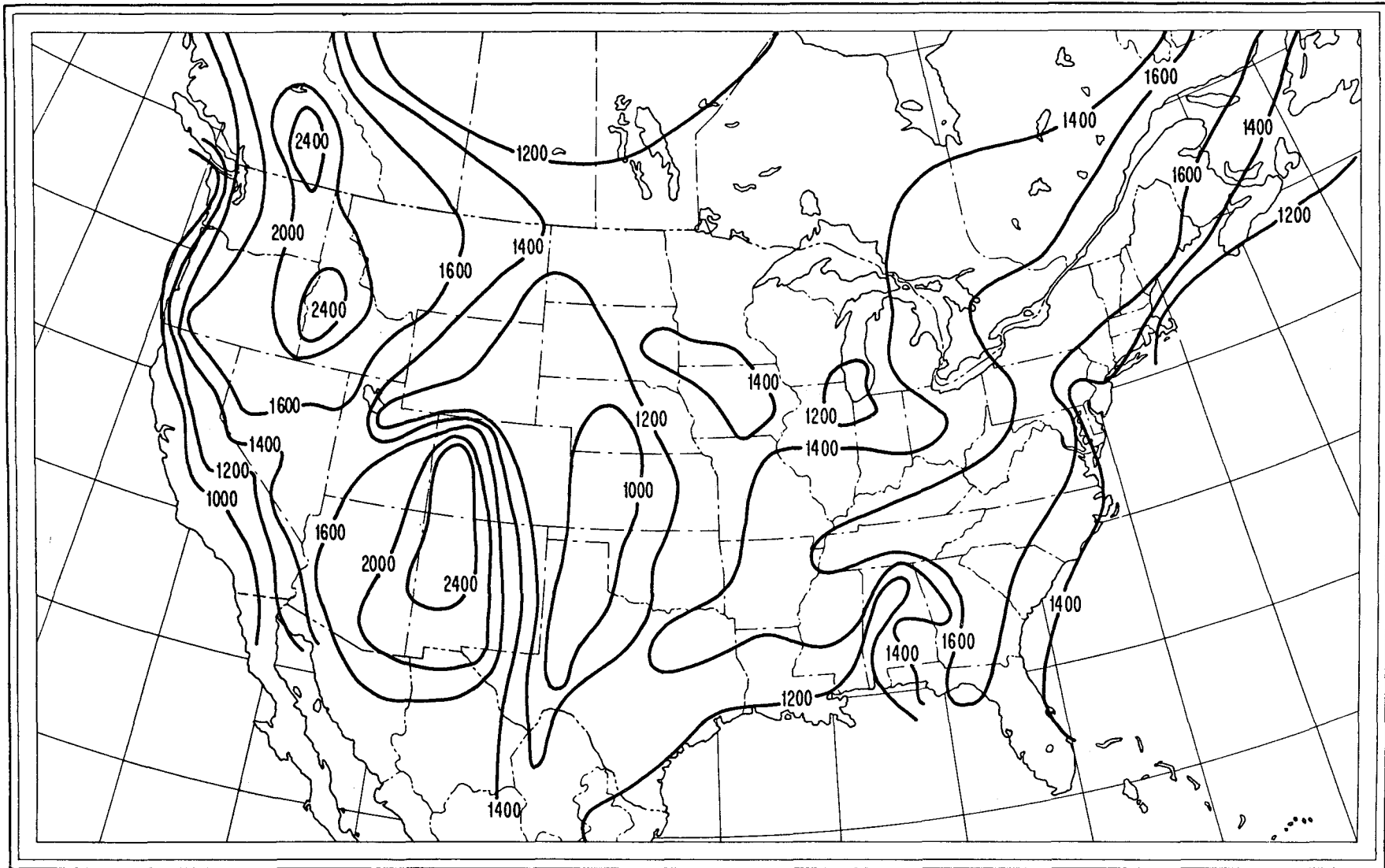


Figure 14. The median base height of elevated ducts, $h_b(50\%)$ in meters above the surface.

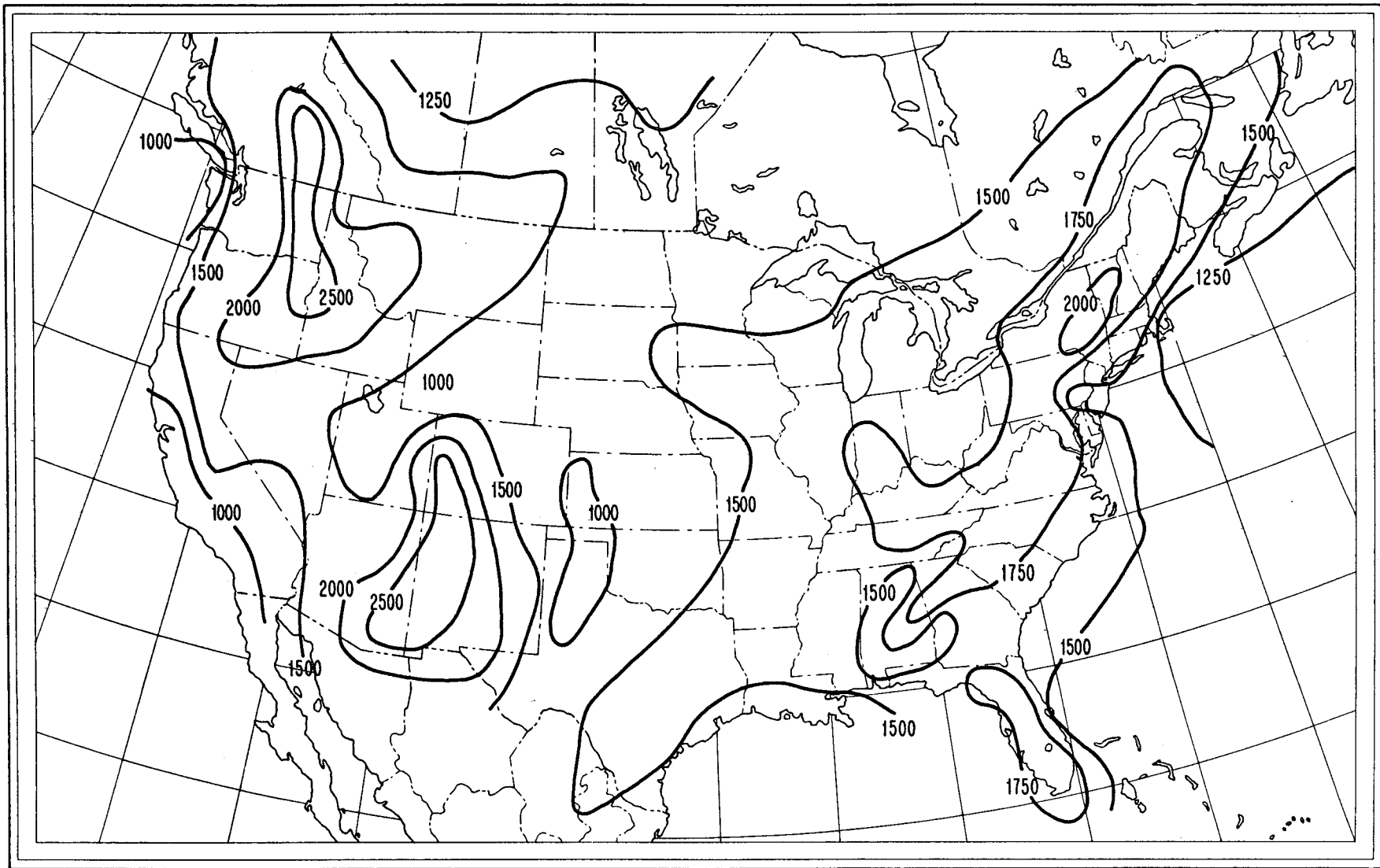


Figure 15. The median elevation of the top of elevated ducts, $h_a(50\%)$ in meters above the surface.

From (2b), for $p = 1\%$ of the time

$$\begin{aligned} \frac{dM}{dh} &= -1570 + 157 = -1413 \text{ M units/km} \\ &= -1.413 \text{ M units/m.} \end{aligned} \quad (11c)$$

From (3b),

$$\delta M = -1.413(10) = -14.13 \text{ M units.} \quad (11d)$$

From (3a),

$$2\theta_c = 2 \sqrt{2(14.13)} = 10.63 \text{ mrad} = 0.61^\circ. \quad (11e)$$

From (10) for $\Omega \geq 10.63 \text{ mrad}$,

$$\begin{aligned} A_c &= -10 \log (10.63/\Omega) \\ &= -10.27 + 10 \log \Omega. \end{aligned} \quad (11f)$$

For both terminals immersed in the surface duct ($h_T, h_R < 100 \text{ m}$ at most), the basic transmission loss for a 145 km path at 0.53 GHz is given by (8) for $p = 1\%$ of the time as

$$\begin{aligned} L_b(1\%) &\geq 92.45 + 20 \log(0.53) + 10 \log(145) + 0.03(145) \\ &\quad - 20.54 + 10 \log \Omega_T + 10 \log \Omega_R \end{aligned}$$

or

$$L_b(1\%) \geq 92.36 + 10 \log \Omega_T + 10 \log \Omega_R. \quad (12)$$

Unless the beamwidths exceeds a few degrees, this duct basic transmission loss will be less than the free-space basic transmission loss of (9),

$$L_{b0} = 92.45 + 20 \log(0.53) + 20 \log(145) = 130.16 \text{ dB.} \quad (13)$$

4.1 Application to Broadcasting

Consider a broadcasting station (or the base station of a land-mobile system) operating in the vicinity of Flint, Michigan, in the 0.45 to 1.0 GHz frequency range. From Figures 8 and 9, we note that elevated ducting layers occur in the Flint area for about 18% of the year, but for about 45% of the worst month (August). The median minimum trapping frequency, from Figure 11, is about 0.4 GHz. That is, interference signals at $f > 0.4 \text{ GHz}$ could be supported via elevated layers for about $0.5(18\%) = 9\%$ of the year or about $0.5(45\%) = 22\%$ of August.

Let us assume the system parameter values

$$\begin{aligned} f &= 0.53 \text{ GHz}, \quad \Delta H = 50 \text{ m}, \\ h_T &= 75 \text{ m}, \quad \Omega_T = 10^\circ \text{ or } 174.5 \text{ mrad}, \\ h_R &= 10 \text{ m}, \quad \Omega_R = 45^\circ \text{ or } 785.4 \text{ mrad}. \end{aligned} \quad (14)$$

where f is the transmission frequency, ΔH is a measure of terrain irregularity (the 10% to 90% range of elevations at 10 to 50 km from the transmitter [CCIR, 1978a]), the h_T and h_R are the heights of the transmitting and receiving antenna centers of radiation in meters above some common reference elevation, and the Ω_T and Ω_R are the transmitting and receiving antennas vertical-plane half-power beamwidths. At a distance of $d = 145$ km, the basic transmission loss for surface duct propagation is, from (12) and (14),

$$L_b(1\%) \leq 92.36 + 10 \log(174.5) + 10 \log(785.4) = 143.73 \text{ dB}. \quad (15)$$

In the case of elevated ducts, we note from Figure 14 that the median elevated-duct base height is $h_b(50\%) > 1400$ m so that both terminals given by (14) are positioned below the elevated duct. By means of energy coupled into and out of non-uniform elevated ducts, as mentioned in the paragraphs following (10) in job-section 2.5, an upper bound on the basic transmission loss for a field at a distance of 145 km would be given by

$$L_b(9\%) \leq L_{b0} + 10 + 10 = L_{b0} + 20 \text{ dB}. \quad (16)$$

From (13) and (16)

$$L_b(9\%) \leq 130.16 + 20 = 150.16 \text{ dB}. \quad (17)$$

The foregoing values of basic transmission loss may be related to estimates of the corresponding field strengths by

$$20 \log [E_0/E(p)] = L_b(p) = L_{b0} \text{ dB}, \quad (18)$$

for the expected ducted fields expressed in decibels below the free-space field. That is, from (13), (15), (17), and (18),

$$20 \log [E_0/E(1\%)] = 143.73 - 130.16 = 13.57 \text{ dB}(E_0) \quad (19a)$$

$$20 \log [E_0/E(9\%)] = 150.16 - 130.16 = 20 \text{ dB}(E_0). \quad (19b)$$

For the parameter values of (14), the CCIR [1978g] provides predicted broadcast fields for both the standard condition (50% of all locations for 50% of the time) and for selected percentages of the time (50% of all locations for $p = 10\%$ and 1% of the time). For paths over either the Mediterranean Sea or overland (at roughly the same North latitudes as the Great Lakes), Table I lists the calculated fields, from (19a) and (19b), and the empirical CCIR predictions. For mixed land/sea paths, the CCIR recommends interpolation on the basis of the proportion of the oversea to total path lengths.

Table 1. Comparison of Broadcast Fields in Decibels Below the Free-Space Level at Flint, Mich., for 50% of Receiver Locations 450 to 1000 MHz.

p % of the time	CCIR (overland, $\Delta H = 50$ m)		Calculated $20 \log [E_0/E(p)]$
	$20 \log [E(p)/E(50\%)]$	$20 \log [E_0/E(p)]$	
1	14 dB	45 dB	13.6 dB
10 *	7	52	20.0
50	0	59	--

* approximately, 9 and 10%

The first column of Table 1 is the percent of the year. The second column is the empirically expected service field level relative to the median (50%) field; this indicates modest field enhancements for 10% and 1% of the time. The third column is the same listing of service fields, but expressed in decibels below the free-space level. The third column should be compared with the fourth column values of interference fields to see the effect on overland paths when there are more horizontally extensive elevated ducts present. These fourth column fields exceed those of the third column by the order of 30 dB.

The CCIR predictions of broadcast fields are representative of average climatic conditions throughout the temperate zone [CCIR, 1978g]. As averages of data from broadcast systems of North America, Europe, Japan, etc., they are appropriate for the prediction of service fields. However, for the purpose of protecting against interference, a biased estimate is required [CCIR, 1978h]. One might prefer an estimate from many broadcast systems (of the field exceeded for 1% of the time) based upon the highest observed 1% field, not the average observed 1% field. Table 1 illustrates the inadequacy of estimating interference fields (highest 1% fields), by service-field (average 1% fields) prediction methods.

5. RECOMMENDATIONS

The preceding text, particularly its referenced material, demonstrates the feasibility of predicting interference fields. The next step would be the development of more complete prediction procedures. Advances are required in four aspects of the problem:

- (a) additional experimental studies,
 - (b) further theoretical developments,
 - (c) formulation of more complete engineering expressions,
- and (d) an improved historical data base.

Let us now discuss these four items in further detail:

(a) Additional experimental studies are required to specify further the horizontal periodicity of elevated ducting layers [Crane, 1980] to determine which aspects of that structure contribute to the efficient coupling of energy into and out of the duct from above or below. Is the periodicity simply D , that of a horizontal sinusoidal structure with distance, $h_0(x) = h_0(o) + c \sin(2\pi x/D)$, that has been occasionally observed by the Acoustic or FM-CW Radars [Hall, 1971; Richter, 1969]? Is the periodicity more subtle, such as $\delta M = \delta M_0 \sin(2\pi x/D)$ or $\delta h = \delta h_0 \sin(2\pi x/D)$? Are there internal variations of structure that would complicate ducting behavior at EHF and higher frequencies?

(b) Further theoretical progress is required. In the case of horizontally uniform layers, some rudimentary but encouraging developments have raised the possibility of associating the various modal (full-wave) solutions with particular wave-trajectories (ray tracing) [Cho et al., 1979; Migliora et al., 1980; Ott, 1980]. Probably, further developments in wave trajectory characteristics will be required (Appendix A) before the mode/ray association will mature and permit extension to nonuniform-duct propagation. Further development of theoretical solutions is required for horizontally non-uniform layers. The non-uniform structures of interest, in addition to the already treated piecewise continuous ducts [Cho and Wait, 1978], are those for horizontally continuously changing layer thicknesses or refractivity gradients and whatever structures are developed under (a) above.

(c) Formulation of more complete engineering expressions would proceed rapidly if a general relationship between the modal (full-wave) solutions and wave-trajectory solutions can be developed. This would permit the accommodation of antenna patterns, polarization, the localized proximity of irregular terrain boundaries, and irregular atmospheric stratification; these are so necessary to the system design engineer.

(d) An improved historical data base would be readily achieved by an expansion of the data base, a refinement of the data base, and the spatial and temporal

extrapolation of the data base. Expansion of the data base would involve the incorporation of much more than the present three years of data -- at least 20 to 30 years of data -- to determine the mean (or median), annual or worst-month parameter distribution of characteristics and their year-to-year variation. If the year-to-year temporal distributions are well behaved, their standard deviation about median-year values would probably suffice. Initially, this need not be carried out for all 107 stations in the United States; one would start with the data from a dozen selected representative stations.

A refinement of the data base would require some modification of the successful data-reduction procedures employed to date. The modifications would be to obtain better estimates of the elevated-layer refractivity gradients and their vertical extents. They would attempt estimates of lag coefficients to correct for the time-sequential temperature/humidity recordings for rising sensors with finite response characteristics [Bean and Cahoon, 1961; Bean and Dutton, 1961; Dougherty et al., 1967].

A spatial and temporal extrapolation of the proposed improved data base is implied when data from twice-a-day soundings at fixed locations are used to estimate the occurrence of ducting layers over twenty-four hours and in a region hundreds of miles square. The diurnal variation of surface and elevated layers should be characterized at select locations in the United States. For example, the data from refractometer soundings recorded over U.S. locations such as the Great Lakes [Bean, 1979], should be compared with the same-day radiosonde data from nearby weather stations. Similarly, the data from "adjacent" U. S. weather stations should be compared.

The above four aspects requiring further study are likely to proceed in independently, but not isolated efforts. However, they may not be able to proceed expeditiously. The referenced investigators are likely to be interested in continuing their efforts, but they may require encouragement by financial and other support. Their interest, demonstrated ability, and need for support should be matched to the urgent requirements expressed at the GWARC-79 [ITU, 1979] for data on ducting and interference fields. These requirements also exist for the U. S. National Radio Regulators (the FCC and NTIA).

6. REFERENCES

- Bahar E., and J.R. Wait (1965), Propagation in a model terrestrial waveguide of non-uniform height: theory and experiment, J. Res. NBS 69D, V No. 11, November, 1445-1463.
- Bean, B.R. (1979), Comment on evaluation of evaporation from Lake Ontario during IFYGL by a modified mass transfer equation, Water Resources Research 15, No. 3, 731.
- Bean, B.R. and B.A. Cahoon (1961), Limitations of radiosonde punch-card records for radiometeorological studies, J. of Geophysical Res. 66, No. 1, January, 328-331.
- Bean, B.R., B.A. Cahoon, C.A. Samson, and G.D. Thayer (1966), A world atlas of atmospheric radio refractivity, ESSA Monograph 1, NTIS Access No. AD-648-805.*
- Bean, B.R., and E.J. Dutton (1961), Concerning radiosondes, lag constants, and radio refractive index profiles, J. of Geophysical Res. 66, No. 11, November, 3717-3722,
- Bean, B.R., R.E. McGavin, R.B. Chadwick, and B.D. Warner (1971), Preliminary results of utilizing the high resolution FM radar as a boundary-layer probe, Boundary Layer Meteorology 1, 446-473.
- Cahoon, B.A., and L.P. Riggs (1964), Climatology of elevated superrefractive layers arising from atmospheric subsidence, Proc. World Conference of Radio Meteorology, Boulder, CO. (American Met. Soc., Boston, MA).
- CCIR (1978a), Report 715, Propagation by diffraction.**
- CCIR (1978b), Report 238-3, Propagation data required for trans-horizon radio-relay systems.**
- CCIR (1978c), Report 724, Propagation data for the evaluation of coordination distance in the frequency range 1 to 40 GHz.**
- CCIR (1978d), Recommendation 525, Calculation of free-space attenuation.**
- CCIR (1978e), Report 719, Attenuation by atmospheric gases.**
- CCIR (1978f), Report 718, Effects of tropospheric refraction of radiowave propagation.**
- CCIR (1978g), Annex of Recommendation 370-3, VHF and UHF Propagation curves for the frequency range from 30 MHz to 1000 MHz.**
- CCIR (1978h), Report 569-1, The evaluation of propagation factors in interference problems at frequencies greater than 0.6 GHz.**
- Cho, S.H., and J. R. Wait (1978), EM wave propagation in a laterally non-uniform troposphere, Radio Science 13, No. 2, March-April, 253.

* National Technical Information Service (NTIS), 5285 Port Royal Road, Springfield, VA 22161.

** Vol. V., Propagation in Non-Ionized Media, CCIR XIV Plenary Assembly, Kyoto, Japan. Available from NTIS*, Access. No. PB 298-025/PG.

- Cho, S.H., C.G. Migliora, and L.B. Felsen (1979), Hybrid ray-mode formulation of propagation in a tropospheric duct, Session F-6, Proc. URSI/USNC Nat'l Radio Science Mtg., U. of Washington, Seattle, Wash., 18-22 June.
- Crane R.K. (1981), A review of transhorizon propagation phenomena, to appear in the March-April issue of Radio Science.
- Dougherty, H.T. (1968), A survey of microwave fading mechanisms, remedies, and applications, ESSA Tech. Report ERL 69-WPL4, NTIS Access Number COM-71-50288.*
- Dougherty, H.T., and B.A. Hart (1976), Anomalous propagation and interference fields, Office of Telecommunications Report 76-107, NTIS Access No. PB-262-477.*
- Dougherty, H.T., and B.A. Hart (1979), Recent progress in duct propagation predictions, IEEE Trans. Ant. Prop. AP-27, No. 4, July, 542-548.
- Dougherty, H.T., and W.J. Hartman (1977), Performance of a 400 Mbit/s system over a line-of-sight path, IEEE Trans. Comm. COM-25, No. 4, April, 427-432.
- Dougherty, H.T., R.E. McGavin, and R.W. Krinks (1970), An experimental study of atmospheric conditions conducive to high radio fields, Office of Telecommunications Report OT/ITSRR4, (available from NTIS under Access No. COM-75-11138/AS).*
- Dougherty, H.T., L.P. Riggs, and W.B. Sweezy (1967), Characteristics of the Atlantic Trade Wind System significant for radio propagation, ESSA Tech. Report IER 29-ITSA29, (NTIS Access No. AD-651-541).*
- Gossard, E.E. (1962), The reflection of microwaves by a refractive layer perturbed by waves, IRE Trans. AP-10, No. 3, May, 317-325.
- Gossard, E.E., and J.H. Richter (1970), The shape of internal waves of finite amplitude from high-resolution radar sounding of the lower atmosphere, J. Atmospheric Sciences 27, No. 6, Sept., 971-973.
- Gough, M.W. (1962), Propagation influence in microwave link operation, Institute of Radio Engineers (U.K.) 24, July, 53-72.
- Hall, F.F., Jr. (1971), Acoustic remote sensing of temperature and velocity structure in the atmosphere, Statistical Methods and Instrumentation in Geophysics, A.G. Kjelaas (Ed.), Oslo, Sweden: Teknologisk Forlag A/S.
- Hall, M.P.M. (1968), Further evidence of VHF propagation by successive reflections from an elevated layer in the troposphere, Proc. IEE 115, No. 11, 1595-1596.
- Hall, M.P.M. (1980), Effects of the Troposphere on Radio Communications, IEE Electromagnetic Waves Series, #8, Peter Peregrinus LTD, Stevenage, UK.
- Hall, M.P.M., and C.M. Comer (1969), Statistics of tropospheric radio refractive-index soundings taken over a three-year period in the United Kingdom, Proc. IEE 116, No. 5, May, 685-690.
- ITU (1976), Radio Regulations, Vols. I and II, (ISBN 92-61-00181-5), International Telecommunication Union, Geneva, Switzerland.

* National Technical Information Service (NTIS), 5285 Port Royal Road, Springfield, VA 22161.

- ITU (1979), Final Acts of the World Administrative Radio Conference, Vols. I and II, International Telecommunications Union, Geneva, Switzerland.
- Kerr, D.E. (1951), Propagation of short radio waves, Chap. 1, Radiation Laboratory Series, Vol. 13 (McGraw Hill Book Company, Inc., New York, NY). Also available in paperback (Dover, Inc., New York, NY).
- Majumdar, S.C., S.K. Sarkar, and A.P. Mitra (1977), Atlas of tropospheric radio refractivity over the Indian sub-continent, National Physical Laboratory, New Delhi, India.
- Migliora, C.G., S.H. Cho, and L.B. Felson (1980), Hybrid ray-mode analysis of propagation in an elevated tropospheric duct, Proc. URSI Comm. F Open Symposium, Lennoxville, Quebec, 761-7.
- Millington, G. (1957), The concept of the constant radius of the earth in tropospheric propagation, Marconi Rev. 20, No. 126, 79-93.
- Neesen, J., and J. deHaas (1980), Measured statistics of transmission loss due to ducting on transhorizon links at 6.4 and 7.4 GHz, Proc. URSI-F Symposium, Quebec, Canada.
- NTIA (1979), Manual of Regulations and Procedures for Federal Radio Frequency Management, U.S. Dept of Comm., National Telecommunications and Information Administration, 1325 G. St. N.W., Wash., DC 20005.
- Ott, R.H. (1980), Roots of the modal equation for EM wave propagation in a tropospheric duct, J. of Math. Physics 21, No. 5, May, 1256-1266.
- Richter, J.H. (1969), High resolution tropospheric radar sounding, Radio Sci. 4, No. 12, December, 1261-1268.
- Samson, C.A. (1975), Refractivity gradients in the northern hemisphere, Office of Telecommunications Report 75-59, NTIS Access No. COM-75-10776/AS.*
- Saxton, J.A. (1951), The propagation of meteorological waves beyond the horizon, Proc. IEE, 98, Pt. III, 360-369.
- Segal, B., and R.E. Barrington (1977), Tropospheric refractivity atlas for Canada, CRC Report 1315, Dept. of Communications, Ottawa, Canada.
- Wait, J.R. (1962), Electromagnetic waves in stratified media, Chaps. XI and XII (Pergamon Press, New York, NY). There is also a second edition, 1970.
- Wait, J.R. (1964), A note on the VHF reflection from a tropospheric layer, Radio Sci. 68D, No. 7, July, 847-848.
- Wait, J.R. (1969), Reflection from subrefractive layers, Electronic Letters 5, No. 4, February 20, 64-65.
- Wait, J.R., and K.P. Spies (1969), Internal guiding of microwaves by an elevated tropospheric layer, Radio Sci. 4, No. 4, April, 319-326.

* National Technical Information Service (NTIS), 5285 Port Royal Road, Springfield, VA 22161.

APPENDIX A: DUCTING EXPRESSIONS

Millington [1957] showed that a radio wave trajectory within a layer of constant refractivity gradient may be closely approximated by a parabolic arc. His results can be expressed as

$$y(x) = x\theta_0 + x^2 G/2 \quad \text{m,} \quad (\text{A1})$$

$$\theta(x) = \theta_0 + xG \quad \text{mrad,} \quad (\text{A2})$$

$$G = [g + 157] 10^{-3} \quad \text{M units/m.} \quad (\text{A3})$$

The $0 \leq y \leq \delta h$ of (A1) gives the height of a point on the wave trajectory in meters above the layer base elevation (h_0 in Figures 5 and 6) and at a distance of x kilometers from the origin ($y = 0, x = 0$). Note that (A1) is relative to the layer base, regardless of its shape; its shape may change as the layer is arched or flat, but the equation is unchanged. Equation (A2) determines the elevation angle along the wave trajectory in milliradians and is the derivative (with respect to x) of (A1) for the small-angle approximation $\theta(x) \approx \tan \theta(x)$. The layer's modified refractivity gradient $G = G_0 < 0$ M units/m would be determined by (A3) from the layer's ducting refractivity gradient $g_0 < -157$ N units/km. For that portion of the duct below the ducting layer, then $y(x) = h(x) - h_0 \leq 0$, where $h_b \leq h(x) \leq h_0$. The modified refractivity gradient $G = G_b > 0$ M units/m is also determined from (A3), but for a refractivity gradient $g_b > -157$ N units/km. Commonly,

$$G_b = [-40 + 157] 10^{-3} = 0.117 \quad \text{M units/m.} \quad (\text{A4})$$

By manipulation of (A1), (A2), and (A3), several of the trajectory characteristics may be determined. For example, the maximum take-off angle (at $x = 0$) for a trapped trajectory is known as the critical take-off angle

$$\theta_c = \pm \sqrt{2|\delta M|} \quad \text{mrad,} \quad (\text{A5})$$

where the choice of sign is such as to maintain θ_c/G positive. In (A5),

$$\delta M = G_0 \delta h < 0 \quad \text{M units,} \quad (\text{A6})$$

and δh is the ducting-layer thickness in meters. The duct thickness is, from (6),

$$D = \delta h [1 - G_o/G_b] \quad \text{m.} \quad (\text{A7})$$

For an initial elevation angle θ_o at $y = 0$, the wave trajectory parabolic arc within the layer will have, from (A2), a maximum elevation \hat{y} at

$$\hat{x} = -\theta_o/G_o \quad \text{km,} \quad (\text{A8})$$

and

$$\hat{y} = \theta_o \hat{x}/2 = -\theta_o^2/2G_o \quad \text{m.} \quad (\text{A9})$$

Of course,

$$\frac{\hat{y}}{\delta h} = \left(\frac{\theta_o}{\theta_c}\right)^2 \leq 1.0 \quad (\text{A10})$$

At the point $y(x)$,

$$x = \hat{x} [1 \mp Q(x)] \quad \text{km,} \quad (\text{A11})$$

and

$$\theta(x) = \pm \theta_o Q(x) \quad \text{mrad,} \quad (\text{A12})$$

where the choice of sign is the opposite of that for (A11). For example, $\theta(x) > 0$ for $x < \hat{x}$. The $Q(x)$ is given by

$$Q(x) = \sqrt{1 - y(x)/\hat{y}} \quad \text{for } y > 0, \quad (\text{A13})$$

and

$$Q(x) = \sqrt{1-y(x)/\hat{y}_b} \quad \text{for } y < 0, \quad (\text{A14})$$

where

$$\hat{y}_b = \delta h \frac{G_o}{G_b} < 0 \quad \text{m.} \quad (\text{A15})$$

For the trajectory parabolic arc, $y(x) \geq 0$, the chord length from $y(x=0)$ to $y(x=x_{\max}) = 0$ is

$$(x_{\max})_o = 2\hat{x} = -2\theta_o/G_o > 0 \quad \text{km.} \quad (\text{A16})$$

For the trajectory parabolic arc $y(x) \leq 0$, the chord length is given by

$$(x_{\max})_b = - (x_{\max})_o \frac{G_o}{G_b} > 0 \quad \text{km,} \quad (\text{A17a})$$

$$= 2\hat{x}_b = -2\theta_o/G_b > 0 \quad \text{km.} \quad (\text{A17b})$$

APPENDIX B: CONTOUR MAPS FOR 10 AND 90 PERCENTILE VALUES

This appendix contains the upper and lower decile values as bounds for the four duct parameters f_t , h_b , h_o , and h_a .

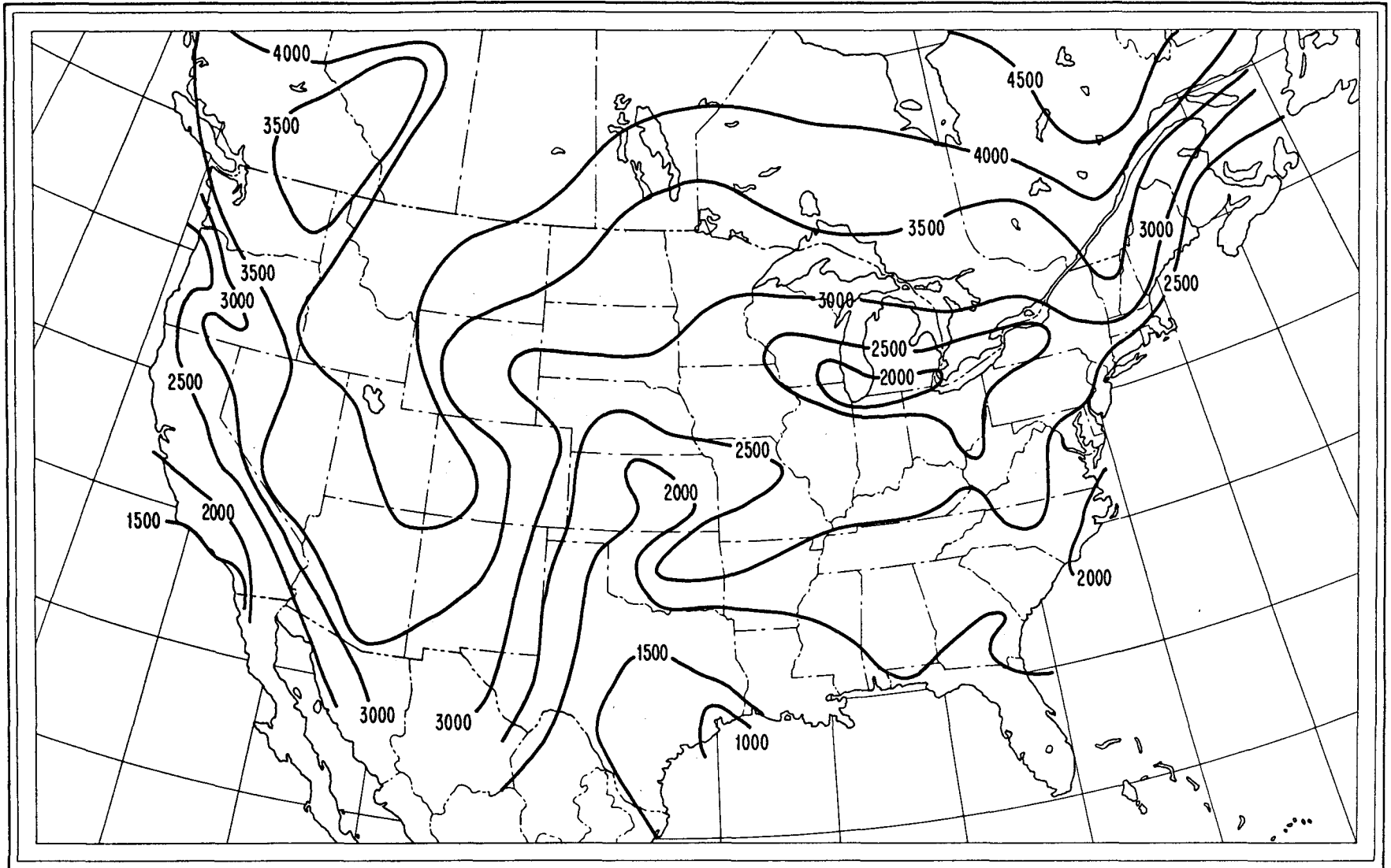


Figure B-1. An upper bound for the minimum trapping frequency, $f_t(10\%)$ in megahertz. Only for less than 10% of elevated ducts would efficient trapping be limited to frequencies exceeding the indicated values.

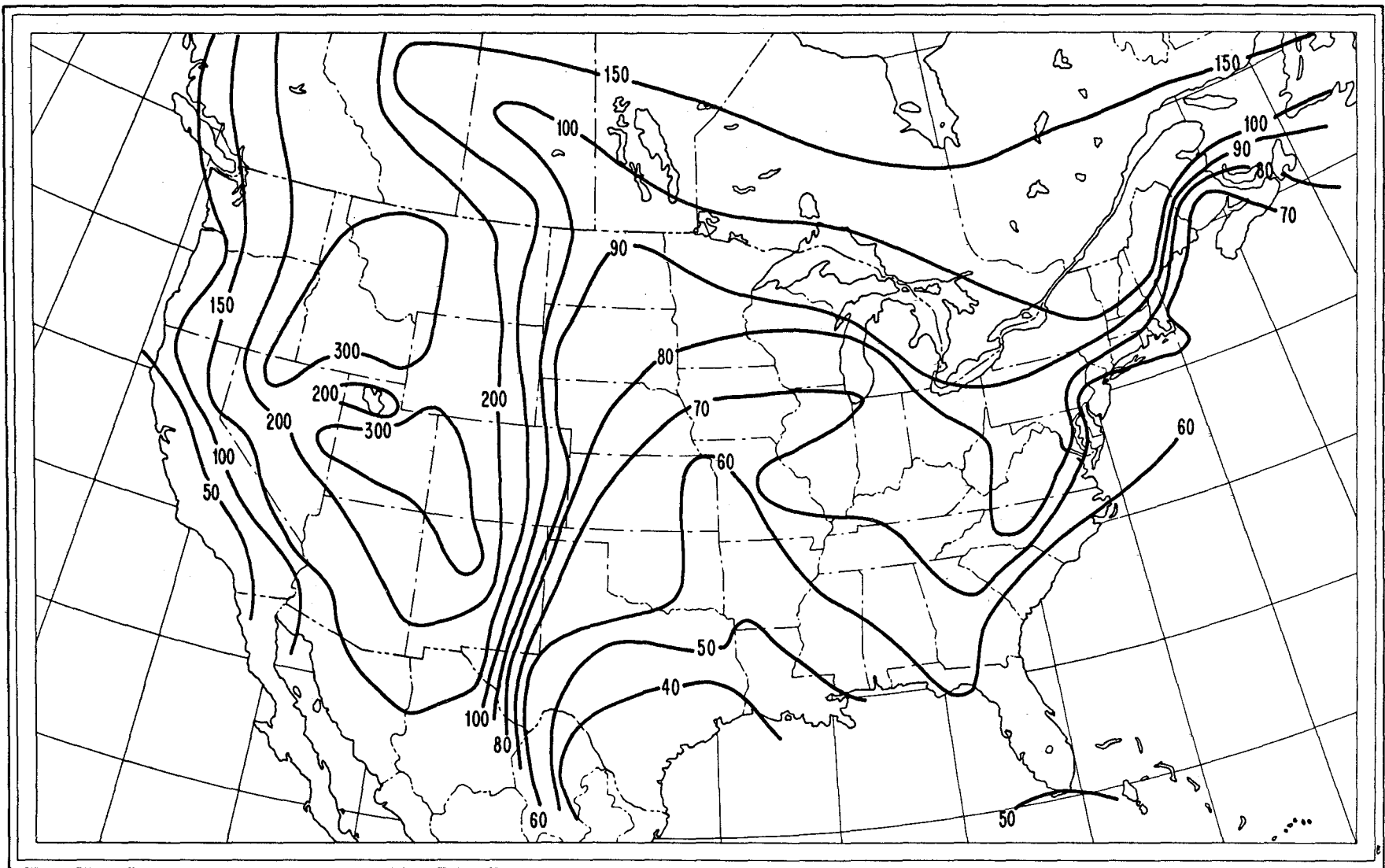


Figure B-2. A lower bound for the minimum trapping frequency, $f_t(90\%)$ in megahertz. For more than 90% of the elevated ducts, efficient trapping could occur for frequencies exceeding the indicated values.

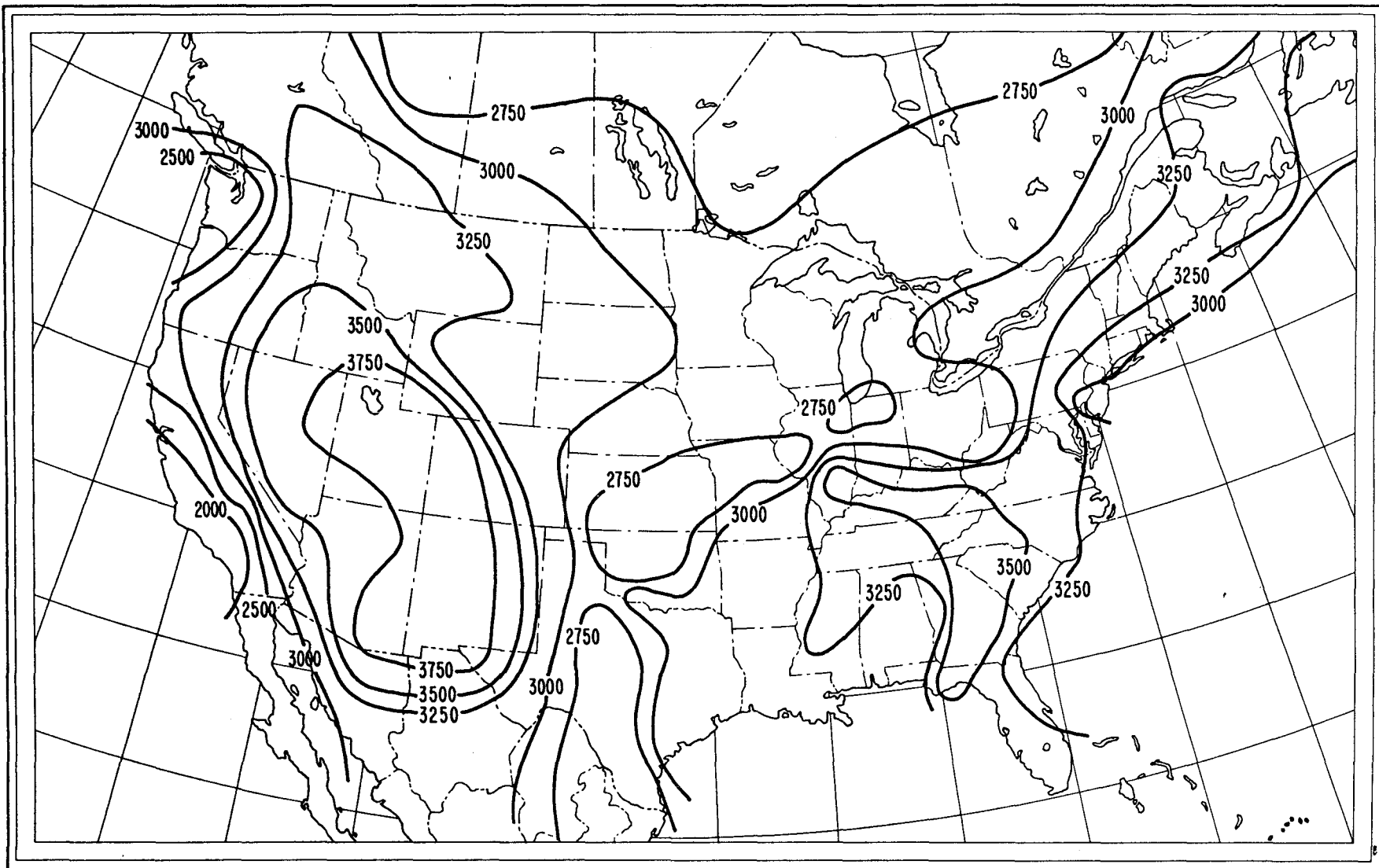


Figure B-3. An upper bound on the base height of the elevated ducts, $h_b(10\%)$ in meters above the surface. For all but 10% of the elevated ducts, the expected base height h_b would not exceed the indicated values.

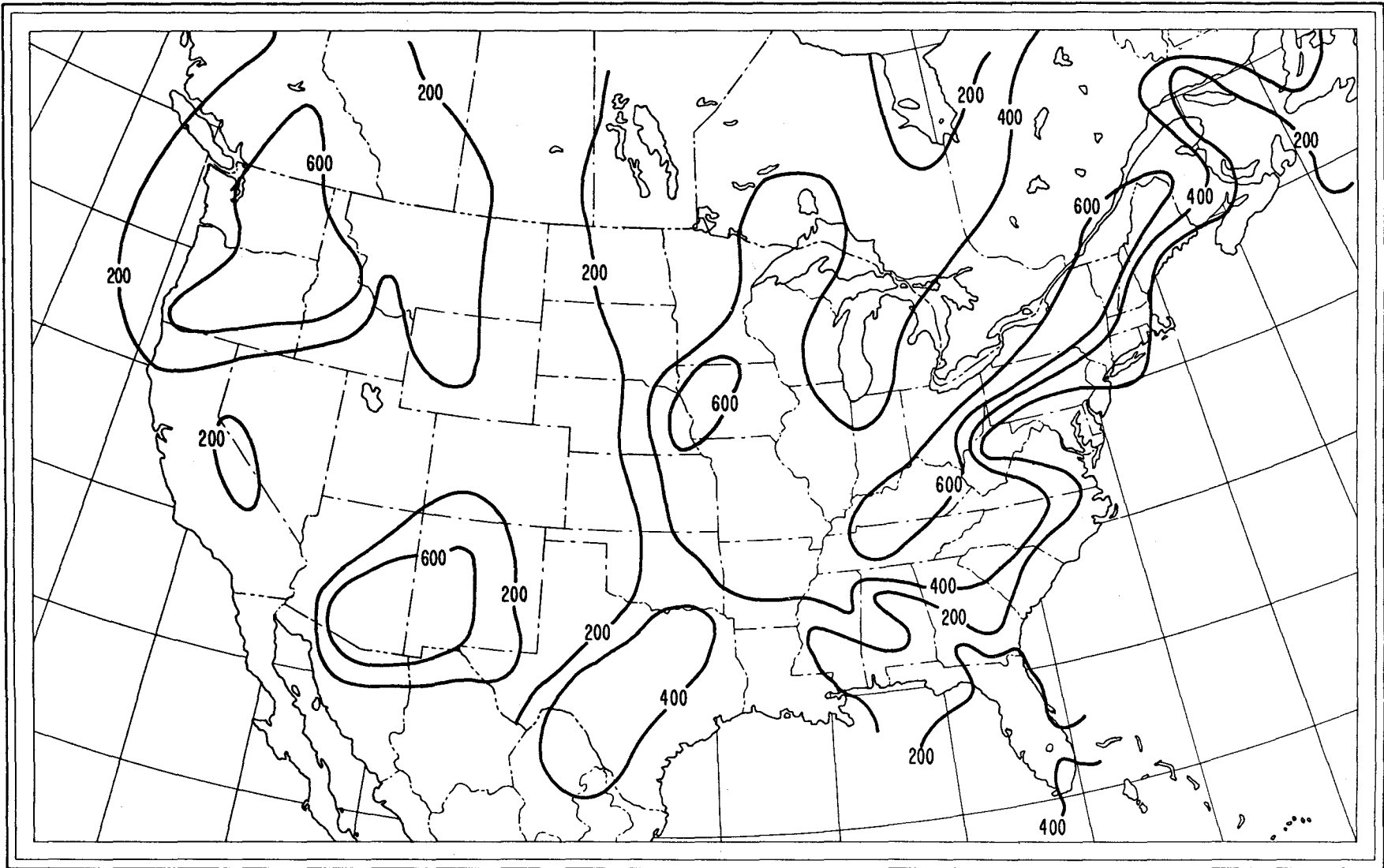


Figure B-4. A lower bound on the base height of elevated ducts, $h_b(90\%)$ in meters above the surface. For 90% of the elevated ducts, the expected height of their base, h_b , would exceed the indicated values.

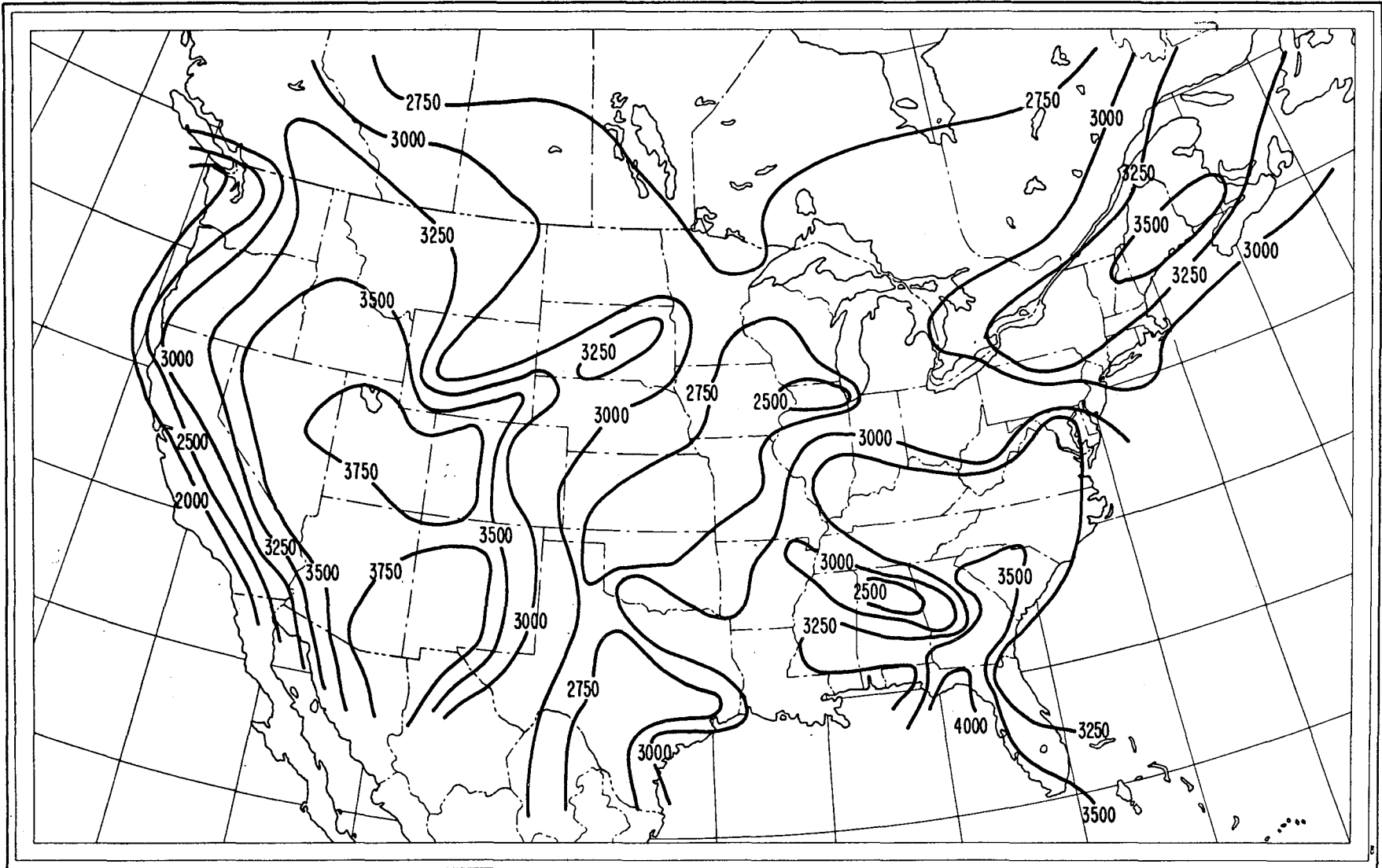


Figure B-5. An upper bound on the optimum coupling elevation, $h_0(10\%)$ in meters above the surface. For all but 10% of elevated ducts, the expected h_0 would not exceed the indicated values.

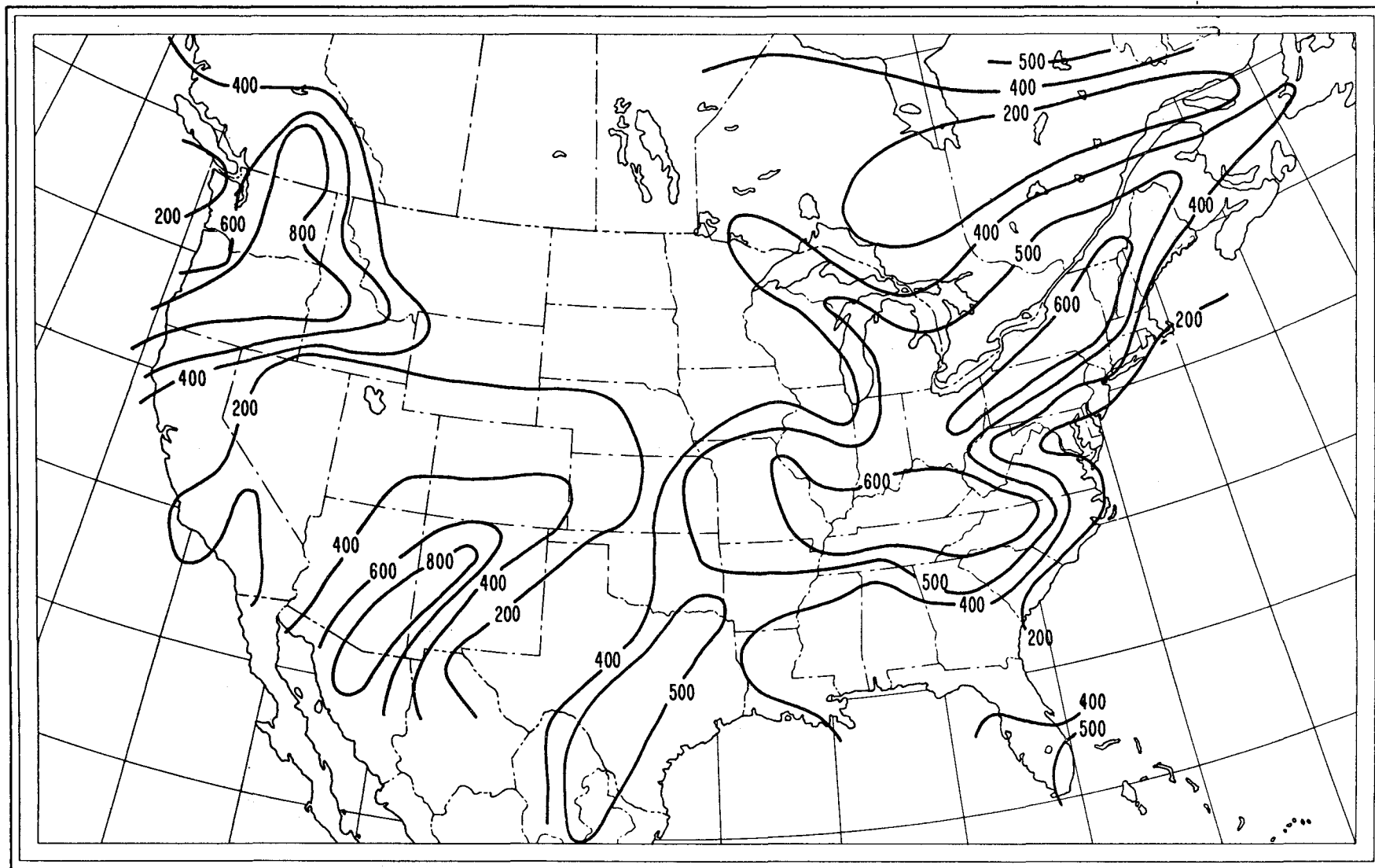


Figure B-6. A lower bound on the optimum coupling elevation, $h_0(90\%)$ in meters above the surface. For 90% of elevated ducts, the expected h_0 would exceed the indicated values.

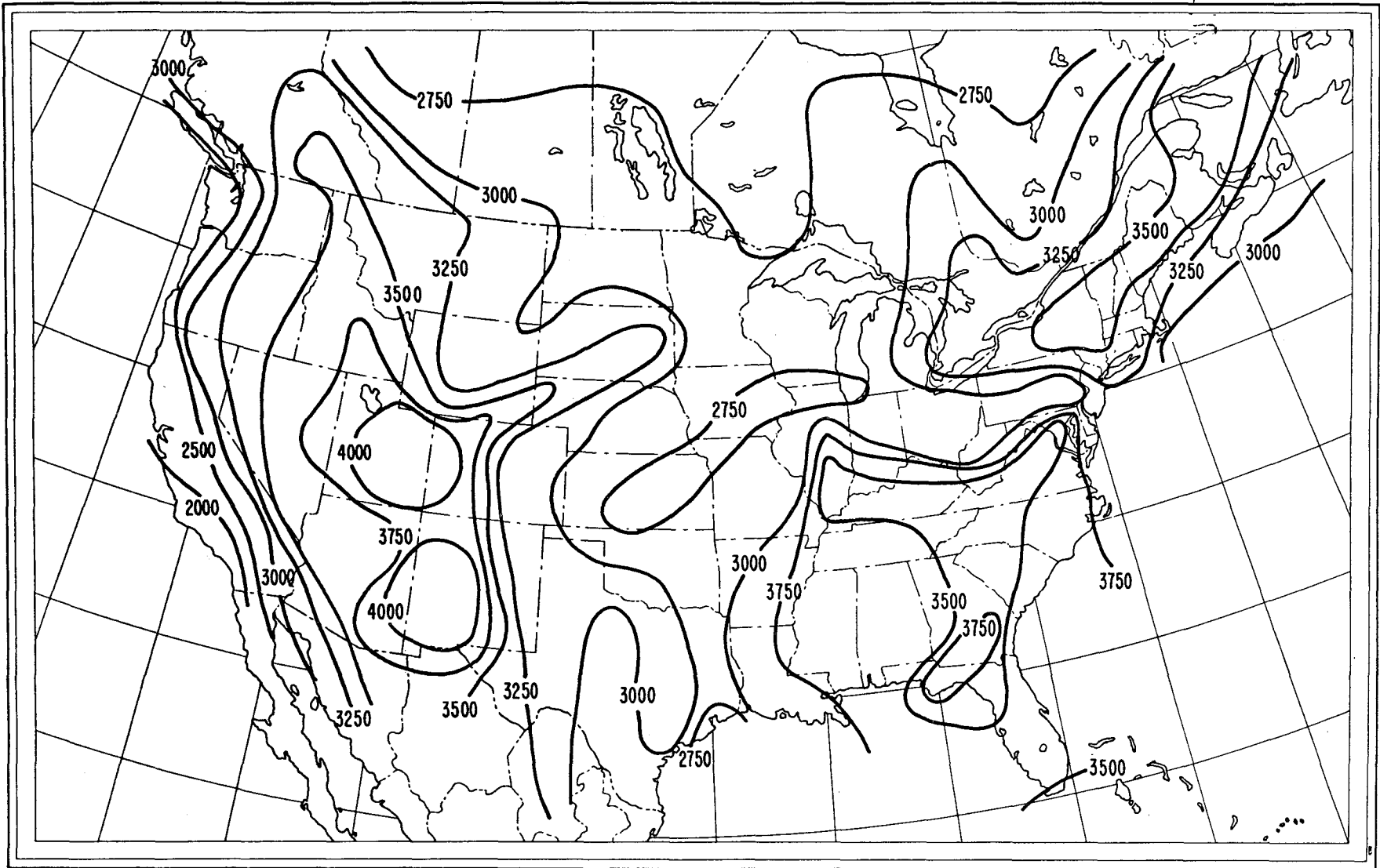


Figure B-7. An upper bound on the elevation at the top of the ducts, $h_a(10\%)$ in meters above the surface. Only for 10% of the ducts would the expected h_a exceed the indicated values.

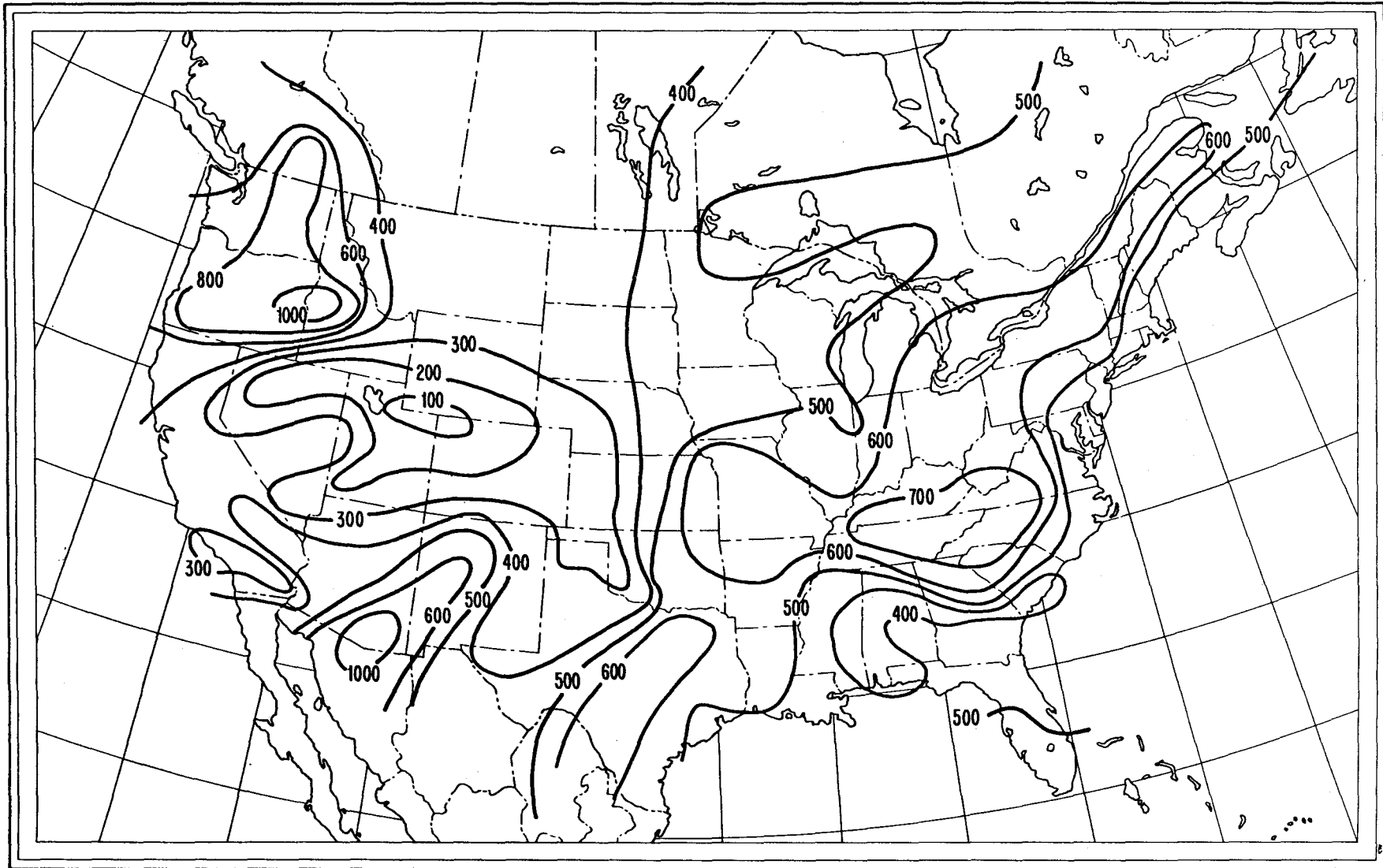


Figure B-8. A lower bound on the elevation at the top of a duct, $h_a(90\%)$ in meters above the surface. For 90% of elevated ducts, the h_a would exceed the indicated values.

APPENDIX C: SCHEMATIC REPRESENTATIONS OF SOME METEOROLOGICAL CONDITIONS
FAVORABLE FOR ANOMALOUS RADIO PROPAGATION

H.T. Dougherty, R.E. McGavin,* and B.A. Hart**

This appendix categorizes for the telecommunications system design engineer, some of the meteorological conditions associated with the atmospheric refractivity (N) layers that are favorable for anomalous radio wave propagation. These layers may be categorized in terms of their position (surface or elevated), their refractivity gradients (subrefractive, superrefractive), and their causative physical processes (advection, evaporation, etc.). These layers are exemplified by simplified plots (straight-line segments) of their refractivity profiles (N versus elevation h), or their associated temperature (T in °C), or relative humidity (RH in %), profiles (i.e., T and RH versus elevation h above the surface). The geographic, synoptic, and generalized surface conditions associated with the occurrence of each type of layer are described qualitatively. In some cases, specific locations are identified as examples.

The layer categorizations are summarized in four charts: Chart I describes surface superrefractive layers ($\Delta N/\Delta h < -100$ N units/km); Chart II depicts surface subrefractive layers ($\Delta N/\Delta h > 0$); Chart III treats elevated superrefractive layers; and Chart IV describes elevated subrefractive layers. When the Chart I layers have sufficiently superrefractive gradients (i.e., ducting gradients where $\Delta N/\Delta h < -157$ N units/km), the surface layer also constitutes a surface radio duct. Elevated refractivity layers with ducting gradients may constitute either elevated or ground-based ducts (See Figure 7 of the text).

* U.S. Department of Commerce, National Oceanic And Atmospheric Administration, Weather Modification Program Office, Boulder, CO 80303

** U.S. Department of Commerce, National Telecommunications And Information Administration, Office of Policy Analysis And Development, Boulder, CO 80303

SOME METEOROLOGICAL CONDITIONS FAVORABLE FOR ANOMALOUS RADIO PROPAGATION

Chart I Surface Superrefractive Layers ($\Delta N/\Delta h < -100$ N-units/km)

CAUSATIVE PROCESS	DESCRIPTION			OCCURRENCE
	N-Profile	T-Profile	RH-Profile	
<p>A ADVECTION</p> <p>Horizontal motion of warm dry air across a cool moist surface (sea or moist ground). The warmer and drier the air, the stronger the gradient.</p>				<p>(1) Over large bodies of water such as lakes, bays, gulfs and seas; particularly along desert coastal regions (e.g., in the Mediterranean and Red seas, the Gulf of Arabia or in the English Channel during summers). The layers have been observed to extend up to 70 meters above the sea surface and out to 20 km from the shore.</p> <p>(2) Over cool irrigated valleys, below hot dry mountain slopes, just after sunset.</p>
<p>B QUASI-ADVECTION</p> <p>Horizontal motion of cool air across a warm moist surface (sea or moist ground). The stronger the wind, the stronger the gradient.</p>				<p>(1) Over the poleward portions of temperate-zone seas in the winter (e.g., the North Atlantic).</p> <p>(2) Over moist land areas near the tropics. (e.g., Florida) during early winter.</p> <p>(3) In temperate-zones following a cold front passage.</p>
<p>C EVAPORATION</p> <p>Evaporation from wet surfaces (sea or moist ground) to air at the same or higher temperatures. The less the wind speed, the stronger the gradient. The warmer the air, the weaker the gradient.</p>				<p>(1) Over land in moist tropical regions, particularly with vegetation and foliage cover and more commonly in the daytime.</p> <p>(2) Over the sea when the air is as warm as or warmer than the sea and in the absence of strong winds.</p> <p>(3) Over the sea in the tradewind regions as a "semi-permanent" layer extending up to 6 to 20 meters.</p>
<p>D FRONTAL WEATHER PROCESSES</p> <p>The advance of cool air along the surface, lifting a stable warm air mass.</p>				<p>Over land in the near vicinity of the front (the junction of the two air masses at the surface)</p>
<p>E RADIATION</p> <p>The radiation of heat from the warmer ground to the colder sky.</p>				<p>Clear skies and light surface winds, at night, result in considerable cooling of the earth causing the formation of a temperature inversion (an increase of temperature with height)</p> <p>Of major importance in the polar regions and during the winter at temperate latitudes where solar heating is confined to a limited surface depth. Probably unusual in tropical regions or in humid regions during the summer.</p>

SOME METEOROLOGICAL CONDITIONS FAVORABLE FOR ANOMALOUS RADIO PROPAGATION

Chart II Surface Subrefractive Layers ($\Delta N/\Delta h > 0$ N-units/km)

CAUSATIVE PROCESS	DESCRIPTION			OCCURRENCE
	N-Profile	T-Profile	RH-Profile	
A ADVECTION Horizontal motion of cool moist air across a dry hot surface.				Over land in coastal regions, during the summer at temperate latitudes. On the eastern coasts in the tradewind regions.
B FRONTAL WEATHER PROCESSES The advance of cool dry air along a warm moist surface, lifting a warm moist air mass.				Over land, with passage of a front so that warm moist air overlies cool air.
C AUTO CONVECTION The convection of heat from an extremely hot surface. Due to cooler air lying above a hot surface (surface temperatures in excess of 30°C due to solar heating) a temperature lapse exists far in excess of the adiabatic temperature lapse rate.				Over land. Encountered in the summer for any desert or semi-arid region (e.g., the interior of Australia, North Africa, the Middle East, the Caspian Sea region and parts of southwestern U.S.). This is rare in winter in the temperate zones.
D CONDUCTION The effect of solar heating of a surface and the heating (conduction) of air near the surface is to cause a sharp increase in air temperature in the immediate vicinity of the surface.				Over land on sunny days during the warm part of the day. This surface boundary layer can occur in any climate and is especially common in tropical deserts and semi-arid climates.
E Process undefined but the effect is a strong elevated superrefractive layer (gradient less than -157 N-Units/km) lying above a subrefractive layer.				Over land. Has been observed in the temperate zones. May occur due to the intrusion of moist air into a dry air mass close to the surface of the ground.

SOME METEOROLOGICAL CONDITIONS FAVORABLE FOR ANOMALOUS RADIO PROPAGATION

Chart III Elevated Superrefractive Layers ($\Delta N/\Delta h < -100$ N-Units/km)

CAUSATIVE PROCESS	DESCRIPTION			OCCURRENCE
	N-Profile	T-Profile RH-Profile		
<p>A <u>ADVECTION</u></p> <p>Horizontal motion of dry air over moist air.</p>			<p>Over land and water near the coast, the subsidence of the dry land air over moist sea air may occur. Daytime solar heating of land surfaces causes a rising of warm dry air near the land and a horizontal motion of moist air from sea to land (sea breeze).</p>	
<p>B <u>SUBSIDENCE</u></p> <p>The flow of air from a high pressure cell such that hot, dry air flows out (subsiding) over cool moist air.</p>			<p>Over water roughly between 5° and 25° North and South latitude, elevated layers occur which are known as the Tradewind Inversion. These are due to subsidence of dry air from high altitudes which subsides over moist cool air over the sea.</p> <p>Over land, the subsidence can occur due to a large slow moving high pressure system associated with the afore-mentioned over-water highs.</p>	
<p>C <u>ADVECTIVE INTRUSION</u></p> <p>The horizontal motion of air, such that one air mass intrudes into another, can produce multiple elevated layers.</p>			<p>WARM MOIST INTRUSION</p> <p>A tongue of warm moist air intruding into a cool dry air mass results in the combination of a superrefractive layer positioned above a subrefractive layer. Observed mainly over land in the temperate zone. Fairly common occurrence.</p> <p>COOL MOIST INTRUSION</p> <p>A tongue of cool moist air intruding into warm dry air produces a similar super/sub type of N profile. Uncommon except possibly in some warm desert areas near cold water coasts.</p>	
			<p>COOL DRY INTRUSION</p> <p>A tongue of cool dry air intruding into a warm moist air mass results in the combination of a subrefractive layer positioned above a superrefractive layer. Observed mainly over land in the temperate zone. Fairly common.</p> <p>WARM DRY INTRUSION</p> <p>A tongue of warm dry air intruding into a cooler moist air mass produces the same sub/super N profile. Common in tropical and subtropic areas.</p>	

SOME METEOROLOGICAL CONDITIONS FAVORABLE FOR ANOMALOUS RADIO PROPAGATION

Chart IV Elevated Subrefractive Layers ($\Delta N/\Delta h > 0$ N-Units/km)

CAUSATIVE PROCESS	DESCRIPTION			OCCURRENCE
	N-Profile	T-Profile	RH-Profile	
<p>A ADVECTION</p> <p>Horizontal motion of cool moist air across a warm dry surface.</p>				<p>Over land, the horizontal motion of cool moist air over warm dry land (e.g. a sea breeze)</p>
<p>B FRONTAL WEATHER PROCESS</p> <p>The advance of cool air along a surface, lifting warm moist air (cold front).</p>				<p>Over land, after passage of a cold front, so that warm moist air overlays cool air. The layers occur up to 50 km behind the front, at altitudes of 1000 km.</p>
<p>C RESIDUAL PROCESS</p> <p>The effects of changes in surface temperatures upon previously developed surface layer.</p>				<p>Over land in the early evening following the daytime formation of auto-convective layers, there is a radiation of heat from ground to clear cool sky and to the moisture trapped above the surface.</p> <p>Over land in the early morning, following a nighttime formation of a radiation layer. Solar heating raises the surface temperature to produce the same elevated subrefractive N profile.</p>

APPENDIX D: LIST OF SYMBOLS

A	general term for excess propagation losses within a duct, in decibels; see (8).
A_c	the aperture-media coupling loss in decibels, see (10).
c	constant of proportionality, see page 30.
d	path length from transmitting site to receiving site in kilometers.
d_o	that portion of a path length, less than d, that lies immersed within a duct.
dn/dh	the vertical refractive index gradient in n units/km, see (1b).
dN/dh	the vertical refractivity gradient in N units/km, see (1b).
dM/dh	the vertical modified-refractivity gradient in M units/km, see (2b).
D	duct thickness in meters, see (4), or (6), and (A7).
E(p)	the field exceeded for p percent of the time, see (18).
E_o	the free-space field, see (18).
f	the radio transmission frequency in gigahertz, see (8), and (9).
f_t	the minimum trapping frequency in gigahertz, see (7); the frequency is expressed in megahertz in Figures 11, B-1, and B-2.
g	the vertical refractivity gradient across an atmospheric layer in N units/km, see (A3).
G	the vertical modified refractivity gradient across an atmospheric layer in M units per meter, M units/m; see (A3).
G_o	the modified refractivity gradient of the ducting layer in M units/m, see (A7).
G_b	the modified refractivity gradient of the non-ducting layer in M units/m, see (A7).
h	the elevation in meters above some reference elevation level.
h_a	the elevation in meters of the top of a ducting layer, see Figure 7.
h_b	the elevation in meters of the base of an atmospheric duct, see Figure 7.
h_o	the elevation in meters of the base of a ducting layer, see Figure 7.
L_b	the basic transmission loss in decibels, see (8).
L_{bo}	the free-space basic transmission loss in decibels, see (9).

$M(h)$	the modified-refractivity profile, see (20).
N	the refractivity profile, see (1a).
$N(h)$	the refractivity profile, see (1a).
$n(h)$	the refractive-index profile, see (1a).
p	the percent of the time.
$Q(x)$	a factor in determining distance and elevation along a wave trajectory, see (A11) through (A14).
R	the subscript to identify receiving terminal parameters, see (14).
R_e	the effective earth radius.
R_0	the true earth radius, $R_0 = 6370$ km.
RH	the relative humidity in percent.
T	the subscript to identify transmitting terminal parameters, see (14).
T	the temperature in degrees centigrade.
x	the distance along a reference elevation level in kilometers, see (A1).
\hat{x}	the distance at which a trajectory has a zero elevation angle, see (A8).
x_{\max}	the maximum distance segment over which an arching (trapped) trajectory will remain within a layer of the duct, the chord length; see (A16).
y	the elevation in meters of a trajectory above a ducting layer base, see Figure 7.
\hat{y}	the peak elevation of a trajectory within a ducting layer, see (A9).
\hat{y}_b	the minimum elevation of a trapped trajectory within a duct, see (A15).
δ	the layer thickness measured in radio wave lengths.
δh	the ducting layer thickness in meters, see (A6), or (A7).
δM	the modified refractivity change through an atmospheric layer in M units/m, see (A5), or (A6).
δM_0	a modified refractivity change used as a reference.
ΔH	a measure of terrain irregularity; the central 10% to 90% range of elevations in meters for the central 90% of the terrain profile between a transmitting and receiving site.
α	a propagation loss coefficient in dB/km for a duct, see

- ρ the reflection coefficient for an elevated layer.
- θ the local elevation angle of a wave trajectory, usually in milliradians; see (A2).
- θ_0 the initial elevation angle of a trajectory in milliradians, see (A1).
- $\hat{\theta}_0$ the initial elevation angle of a trajectory which has a zero elevation angle at the elevation \hat{y} and the distance \hat{x} ; $\hat{\theta}_0 = \theta_c$.
- θ_c the critical initial elevation angle for a duct, see (A5).
- Ω the antenna half-power beam width in milliradians, see (10), directed along a duct; it may represent a sidelobe.

BIBLIOGRAPHIC DATA SHEET

	1. PUBLICATION NO. NTIA Report 81-69	2. Gov't Accession No.	3. Recipient's Accession No.
4. TITLE AND SUBTITLE The Role of Elevated Ducting on Radio Service and Interference Fields		5. Publication Date March 1981	
7. AUTHOR(S) H. T. Dougherty and E. J. Dutton		6. Performing Organization Code NTIA/ITS	
8. PERFORMING ORGANIZATION NAME AND ADDRESS U. S. Department of Commerce National Telecommunications and Information Administration Institute for Telecommunication Sciences Boulder, Colorado 80303		9. Project/Task/Work Unit No.	
11. Sponsoring Organization Name and Address SAME		10. Contract/Grant No.	
14. SUPPLEMENTARY NOTES		12. Type of Report and Period Covered	
15. ABSTRACT (A 200-word or less factual summary of most significant information. If document includes a significant bibliography or literature survey, mention it here.) This report categorizes the manner in which atmospheric stratification can complicate the problems of frequency allocation and radio regulation by inhibiting service fields and enhancing interference fields. For the United States and its border regions, preliminary contour maps are presented for those parameters associated with the atmospheric layering (ducts) conducive to the propagation of unusually strong UHF and SHF fields over extremely long distances. The parameters of interest are: the percent occurrence of elevated ducts, a minimum trapping frequency, the modified refractivity lapse, the ducting-layer base height, the duct-base height, and the duct-top height. The role of these duct parameters in the prediction of potential interference fields is detailed by engineering formulas and illustrated by numerical examples. These predictions of duct characteristics from historical (radiosonde) data are necessarily preliminary because of present inadequacies of the data sample. Approaches for improving estimates of duct parameters are described. Appendices detail expressions for duct trajectories and map the variation of duct characteristics.		13.	
16. Key Words (Alphabetical order, separated by semicolons) anomalous propagation; atmospheric ducts, layers, or stratification; ducting; interference fields; ray trajectories; SHF; UHF			
17. AVAILABILITY STATEMENT <input checked="" type="checkbox"/> UNLIMITED. <input type="checkbox"/> FOR OFFICIAL DISTRIBUTION.		18. Security Class. (This report) Unclassified	20. Number of pages 55
		19. Security Class. (This page) Unclassified	21. Price: